# Dynamic Stability of Delaminated Cross ply Composite Plates and Shells

A THESIS SUBMITTED IN PARTIAL FULFILLMENT OF
THE REQUIREMENTS FOR THE DEGREE OF

**Master of Technology**
**In**
**Structural Engineering**

By

**JAVED ATHER**

**Roll No. 209CE2036**


**DEPARTMENT OF CIVIL ENGINEERING**

**NATIONAL INSTITUTE OF TECHNOLOGY**

**ROURKELA-769008, ORISSA**

**May 2011**

# Dynamic Stability of Delaminated Cross ply Composite Plates and Shells

A THESIS SUBMITTED IN PARTIAL FULFILLMENT OF
THE REQUIREMENTS FOR THE DEGREE OF

**Master of Technology**
**In**
**Structural Engineering**

By

**JAVED ATHER**

**Roll No. 209CE2036**

**Under the guidance of**

**Prof. S. K. Sahu**


**DEPARTMENT OF CIVIL ENGINEERING**

**NATIONAL INSTITUTE OF TECHNOLOGY**

**ROURKELA-769008, ORISSA**

**May 2011**

## ACKNOWLEDGEMENT

It is with a feeling of great pleasure that I would like to express my most sincere heartfelt gratitude to **Prof. S.K Sahu,** Professor, Dept. of Civil Engineering, NIT, Rourkela for suggesting the topic for my thesis report and for his ready and able guidance throughout the course of my preparing the report. I thank you Sir, for your help, inspiration and blessings.

I express my sincere thanks to Director of the institute, **Prof. M. Panda**, Professor and HOD, Dept. of Civil Engineering NIT, Rourkela for providing me the necessary facilities in the department. I would also take this opportunity to express my gratitude and sincere thanks to my honourable teachers **Prof. K.C Biswal, Prof. M.R. Barik, Prof. A.V. Asha** and all other faculty members for their invaluable advice, encouragement, inspiration and blessings. Submitting this thesis would have been a Herculean job, without the constant help, encouragement, support and suggestions from my friends, especially **Itishree Mishra** for their time to help. It will be difficult to record my appreciation to each and every one of them in this small space. I will relish your memories for years to come. I would also express my sincere thanks to laboratory Members of Department of Civil Engineering, NIT, Rourkela.

I must like to thank my **parents** and other **family members**, for their support for choices in all my life and their love, which has been a constant source of strength for everything I do.

**JAVED ATHER**

**ROLL No.- 209CE 2036**


**National Institute of Technology**
**Rourkela**

# CERTIFICATE

This is to certify that the thesis entitled **"DYNAMIC STABILITY OF DELAMINATED CROSS PLY COMPOSITE PLATES AND SHELLS"** submitted by **Mr. JAVED ATHER** in partial fulfillment of the requirements for the award of **Master of Technology** Degree in **Civil Engineering** with specialization in **Structural Engineering** at the National Institute of Technology, Rourkela (Deemed University) is an authentic work carried out by him under my supervision and guidance.

To the best of my knowledge, the matter embodied in the thesis has not been submitted to any other University/ Institute for the award of any degree or diploma.

Date:

**Prof. S.K. Sahu**
**Department of Civil Engineering**
**National Institute of Technology**
**Rourkela – 769008**

# CONTENT

# Abstract:

Fibre reinforced composite plates and shells are increasingly replacing traditional metallic ones. The manufacturing process and service of the composite laminates frequently lead to delamination. Delamination reduces the stiffness and strength of composite laminates because they allow out of plane displacement of plies to occur more easily. Dynamic stability analysis is an integral part of most engineering structures. The present work deals with the study of the effects of free vibration, buckling and dynamic stability of delaminated cross ply composite plates and shells. A first order shear deformation theory based on finite element model is developed for studying the instability region of mid plane delaminated composite plate and shell.

The basic understanding of the influence of the delamination on the natural frequencies, non-dimensional buckling load and non-dimensional excitation frequency of composite plates and shells is presented. In addition, other factors affecting the vibration, buckling and dynamic instability region of delaminated composite plates and shells are discussed.

The numerical results for the free vibration, buckling and dynamic stability of laminated cross-ply plates and shells with delamination are presented. As expected, the natural frequencies and the critical buckling load of the plates and shells decrease with increase in delamination. Increase in delamination also causes dynamic instability regions to be shifted to lower excitation frequencies.

# LIST OF SYMBOL

a, b = Plate dimensions along x- and y-axes, respectively.

[K] = bending stiffness matrix

$[K_g]$ = geometric stiffness matrix

$\omega$ = natural frequency

[M] = mass matrix

{∅} = eigenvectors i.e. mode shape

P = buckling load

$\alpha_0$ = static load factor

$\alpha_1$ = dynamic load factor

$P_{cr}$ = critical buckling load.

$\theta$= Fibre orientation in a lamina

x ,y ,z = System of coordinate axes

t = thickness of plate

u, v, w = Displacement along x, y and z direction.

$N_x$, $N_y$, $N_{xy}$ = In-plane internal force resultants per unit length

$Z_k$, $Z_{k-I}$ = Top and bottom distances of a lamina from the mid-plane

$N_i$ = Shape function at a node i

$K_x$, $K_y$, $K_{xy}$ = Curvatures of a plate

$M_x$, $M_y$, $M_{xy}$ = Internal moment resultants per unit length

$G_{l2}$, $G_{13}$, $G_{23}$ = Shear moduli of a lamina with respect to 1, 2, and 3 axes

$E_1$, $E_2$ = Young's moduli of a lamina along and across fibres, respectively

$Q_x$, $Q_y$ = Transverse shear resultants per unit length

# LISTS OF TABLES

# LISTS OF FIGURE

# CHAPTER 1

# INTRODUCTION

## Introduction:-

Composite laminates are widely used in engineering structures due to their excellent properties, such as high strength-to-weight ratio, high stiffness-to-weight ratio and design versatility etc. Delamination can cause serious structural degradation. Which is a debonding or separation between individual plies of the laminate, frequently occurs in composite laminates. Delamination may arise during manufacturing (e.g., incomplete wetting, air entrapment) or during service (e.g., low velocity impact, bird strikes). They may not be visible or barely visible on the surface, since they are embedded within the composite structures. However, the presence of delamination may significantly reduce the stiffness and strength of the structures and may affect some design parameters such as the vibration characteristic of structure of structure. (e.g., natural frequency and mode shape). Delaminations reduce the natural frequency, as a direct result of the reduction of stiffness, which may cause resonance if the reduced frequency is close to the working frequency. It is therefore important to understand the performance of delaminated composites in a dynamic environment. The subject of predicting the dynamic and mechanical behaviour of delaminated structures has thus attracted considerable attention.

Plate and Shell members have often been used in modern structural systems, because the desired performance can be achieved by controlling the shape of those structures. In particular, high-performance applications of laminated composites to plate and shell members are advantageous because of their light weight, high specific stiffness and high specific strength. However, laminated plates and shells subjected to in plane periodic forces may lead

to dynamic instability for certain combinations of load amplitude and disturbing frequency. Furthermore, plates and shell members with delamination may result in significant changes to their dynamic characteristics. Therefore, it is essential to study the effect of delaminations simultaneously on the dynamic stability of layered shells under periodic loads. Composite plates and shells are widely used in aerospace structures. These are often subjected to defects and damage from both in-service and manufacturing events. Delamination is the most important of these defects

## Importance of the stability studies of delaminated composite shell

Structural elements subjected to in-plane periodic forces may lead to parametric resonance, due to certain combinations of the values of load parameters. The instability may occur below the critical load of the structure under compressive loads over wide ranges of excitation frequencies. Several means of combating resonance such as damping and vibration isolation may be inadequate and sometimes dangerous with reverse results. Structural elements subjected to in-plane periodic forces may induce transverse vibrations, which may be resonant for certain combinations of natural frequency of transverse vibration, the frequency of the in-plane forcing function and magnitude of the in-plane load. The spectrum of values of parameters causing unstable motion is referred to as the regions of dynamic instability or parametric resonance. Thus the parametric resonance characteristics are of great importance for understanding the dynamic systems under periodic loads.

Delamination between plies is one of the most common defects encountered in composite laminates. Delamination can cause serious structural degradation. Which is a debonding or separation between individual plies of the laminate, frequently occurs in composite laminates. Delamination may arise during manufacturing (e.g., incomplete wetting, air entrapment) or

during service (e.g., low velocity impact, bird strikes). They may not be visible or barely visible on the surface, since they are embedded within the composite structures. However, the presence of delaminations may significantly reduce the stiffness and strength of the structures and may affect some design parameters such as the vibration characteristic of structure of structure. (e.g., natural frequency and mode shape). Delaminations reduce the natural frequency, as a direct result of the reduction of stiffness, which may cause resonance if the reduced frequency is close to the working frequency. It is therefore important to understand the performance of delaminated composites in a dynamic environment. The subject of predicting the dynamic and mechanical behaviour of delaminated structures has thus attracted considerable attention.

# CHAPTER 2

# LITERATURE REVIEW

**Introduction:-**Thus the dynamic stability characteristics are of great technical importance for understanding the dynamic systems under periodic loads. In structural mechanics, dynamic stability has received considerable attention over the years and encompasses many classes of problems. The distinction between "good" and "bad" vibration regimes of a structure subjected to in-plane periodic loading can be distinguished through a simple analysis of dynamic instability region. In modelling delamination, both, analytical as well as numerical methods have been used in studying the dynamic and buckling behaviour of composite laminates. Bolotin (1964) in his text on dynamic stability gives a thorough review of the problems involving parametric excitation of structural elements. The dynamic instability of composite plates and shells without delamination has been studied previously by a host of investigators. The studies in this chapter are grouped into three major parts as follows:

- Vibration
- Buckling
- Dynamic stability

The available literature on dynamic stability of delamination composite plates and shells is very limited.

**Free Vibration:**

Tenek (1993) *et al.* studied vibration of delaminated composite plates and some applications to non-destructive testing; he studied the impact of delamination on the natural frequencies of composite plates, as well as delamination dynamics over a broad frequency range, using the finite element method based on the three-dimensional theory of linear elasticity. For the case of cantilever laminated plates, the method is successfully compared with experimental observations.

Lee and Lee (1995) examined the free vibration of composite plates with delamination around cut-outs. They presented a finite element approach is to analyze the free vibration of square and circular composite plates with delamination around internal cut-outs. They presented numerical examples including composite plates with delaminations around circular holes or square cut-outs. And they discussed the effects of the cut-outs and the delamination around the cut-outs on the natural frequencies and mode shapes.

Ju *et al* (1995) presented finite element analysis of free vibration of delaminated composite plates. His study was based on Mindlin plate theory. He presented a finite element formulation for the analysis of the free vibration of composite plates with multiple delamination.

Chang (1998) investigated the vibration analysis of a delaminated composite plate subjected to the axial load. The concept of continuous analysis was used to model the delaminated composite plate as a plate on a discontinuous elastic foundation. The elastic adhesive layer between the buckled composite plate and the undeformed substructure working as a foundation to the plate is represented by linear parallel springs.

Williams and Addessio (1998) studied a dynamic model for laminated plates with delaminations. They presented a dynamic, higher-order theory for laminated plates based on a

discrete layer analysis. The formulation includes the effects of delaminations between the layers of the plate. The model implements a generalized displacement formulation at the lamina level. The governing equations for the lamina are derived using vibrational principles.

Geubelle and Baylor (1998) observed Impact-induced delamination of composites using a 2D simulation. The delamination process in thin composite plates subjected to low-velocity impact is simulated using a specially developed 2D cohesive/volumetric finite element scheme. Cohesive elements are introduced along the boundaries of the inner layers and inside the transverse plies to simulate the spontaneous initiation and propagation of transverse matrix cracks and delamination fronts.

Hou and Jeronimidis (1999) presented vibration of delaminated thin composite plates. He studied experimental (employed free-free vibration system) and finite element modelling of vibration of GFRP laminated circular plates. He shows that the resonant frequencies of low velocity impacted plates are functions of matrix cracking and the local thickening coupling with interlaminar delamination.

Ostachowicz and Kaczmarezyk (2001) studied the vibration of composite plates with SMA fibres in a gas stream with defects of the type of delamination. They analyzed the dynamics of a multi-layer composite plate with delaminations subjected to an aerodynamic load. They proposed finite element model to predict the dynamic response of the system with embedded shape memory alloys (SMA) fibres. They studied the effect of delamination on the natural frequencies of delamination subjected to supersonic flow and determined the flutter instability boundaries.

Hu *et al* (2002) investigated vibration analysis of delaminated composite beams and plates using a higher-order finite element. In order to analyze the vibration response of delaminated composite plates of moderate thickness, he proposed a FEM Model based on a simple higher-

order plate theory, which can satisfy the zero transverse shear strain condition on the top and bottom surfaces of plates.

Chen *et al* (2004) examined the dynamic behaviour of delaminated plates considering progressive failure process. A formula of element stiffness and mass matrices for the composite laminates is deduced by using the first-order shear deformation theory combined with the selecting numerical integration scheme.

Lee and Chung (2010) observed the finite element delamination model for vibrating composite spherical shell panels with central cut-outs. They developed finite element model of vibrating laminated spherical shell panels with delamination around a central cut-out is based on the third-order shear deformation theory of Sanders. In the finite element formulation for the delamination around cut-out, the seven degrees of freedom per each node are used with transformations in order to fit the displacement continuity conditions at the delamination region.

**Static stability:**

Hwang and Mao (2001) investigated failure of delaminated carbon/epoxy composite plates under compression. Their work is to study the buckling loads, buckling modes, postbuckling behaviour, and critical loads of delamination growth for delaminated unidirectional carbon/epoxy composites. Nonlinear buckling analysis, which is a finite-element method including contact elements to prevent the overlapping situation, was applied to predict the delamination buckling loads.

Parhi *et al*. (2001) presented hygrothermal effects on the dynamic behaviour of multiple delaminated composite plates and shells. They presented a quadratic isoparametric finite element formulation based on the first order shear deformation theory for the free vibration

and transient response analysis of multiple delaminated doubly curved composite shells subjected to a hygrothermal environment. For the transient analysis Newmark's direct integration scheme is used to solve the dynamic equation of equilibrium at every time step.

Liu and Yu (2002) studied the Finite element modelling of delamination by layerwise shell element allowing for interlaminar displacements. In his paper, he gave a brief review of the layerwise shell element. He considered geometrically non-linear analysis involving finite rotation and finite strain. According to his results he suggested that central delamination is more damaging than the edge and corner delamination for it causes a greater reduction in the strength and integrity of the plate, in particular in the early stage of shear mode delamination

Shan and Pelegri (2003) investigated the approximate analysis of the Buckling Behaviour of Composites with Delamination. In this paper, they provided an insight into the governing mechanism of the uni-axial compressive buckling of a delaminated composite. They proposed an approximate method to analyse the buckling behaviour as the first step to further investigate the effect of contact zone at the ends of a delamination. The agreement of the analytical results with experiments in critical values of relative axial displacement verifies with his model and approach.

Wang *et al.* (2003) observed Non-Linear Thermal Buckling for Local Delamination near the Surface of Laminated Plates. An investigation is carried out to understand the non-linear thermal buckling behaviour of local delamination near the surface of fibre reinforced laminated plates. The shape of the delaminated region considered is rectangular, elliptic or triangular..

Ju-fen *et al.* (2003) developed reference surface element modelling of composite plate/shell delamination buckling and post buckling. The technique can be easily incorporated into any finite element analysis programme for which the beam, plate and shell elements etc. satisfy the Reissner–Mindlin assumption. They presented the reference surface element formulation

of a four-node $C^o$ quadrilateral membrane-shear-bending element and performed numerical investigations for composite plates and shells with various delamination shapes.

Mümin and KüÇük (2004) investigated the buckling behaviour of simply supported woven steel reinforced thermoplastic laminated plates with lateral strip delamination. He established three dimensional finite element models of the square laminated plates. Each of these models possesses four layers and a different delamination width between the second and third layers. The orientation angle of the fibres is chosen as 0, 15, 30 and 45. He determined the buckling loads for each model having different lateral delamination width.

Tafreshi (2006) examined Delamination buckling and postbuckling in composite cylindrical shells under combined axial compression and external pressure. He investigated the characteristics of the buckling and postbuckling behaviour of delaminated composite cylindrical shells .The combined double-layer and single-layer of shell elements are employed which in comparison with the three dimensional finite elements requires less computing time and space for the same level of accuracy.

Yang and Fu (2006) investigated the Delamination growth of laminated composite cylindrical shells. They derived the post buckling governing equations for the laminated cylindrical shells, based on the variational principle of moving boundary, and the corresponding boundary and matching conditions are given. At the same time, according to the Griffith criterion, the formulas of energy release rate along the delamination front were obtained and the delamination growth was studied.

Oh *et al*. (2008) observed buckling analysis of a composite shell with multiple delaminations based on a higher order zig-zag theory. They developed a new three-node triangular shell element based on a higher order zig-zag theory for laminated composite shells with multiple delaminations. The baseline higher order zig-zag composite shell theory for multiple

delaminations has been developed in a general curvilinear coordinate system and in general tensor notation.

Chirica *et al.* (2010) investigated the buckling analysis of the composite plates with delaminations. In this paper they studied of the influence of elliptical delamination on the changes in the buckling behaviour of ship deck plates made of composite materials is treated. A delamination model has been developed by using the surface-to-surface contact option, in licensed FEM code COSMOS/M. So, the damaged part of the structures and the undamaged part were represented by well-known finite elements (layered shell elements).

Ovesy and Kharazi (2011) observed the stability analysis of composite plates with through-the-width delamination. The analytical method is based on the first-order shear deformation theory, and its formulation is developed on the basis of the Rayleigh-Ritz approximation technique by the implementation of the polynomial series, which has been used for the first time in the case of the mixed mode of buckling.

**Dynamic Stability:**

Radu and Chattopadhyay (2000) analyzed the dynamic stability of composite plates including delamination using higher order theory and transformation matrix. He analyzed composite plates with various thickness and delamination length and placement. Delamination affects the instability regions by shifting them to lower, parametric resonance frequencies and by modifying.

Jinhua and Yiming (2007) studied the analysis of dynamic stability for composite laminated cylindrical shells with delaminations. they derived a set of dynamic governing equations for the delaminated cylindrical shells By introducing the Heaviside step function into the assumed displacement components and using the Rayleigh–Ritz method for minimizing the

total potential energy, Then, the dynamic governing equations are written as the Mathieu-type equations to describe the parametric vibrating behaviour of the shells, and these equations are solved by employing the Bolotin method. They presented numerical results for the dynamic stability of laminated cylindrical shells with delaminations.

Park and Lee (2009) examined parametric instability of delaminated composite spherical shells subjected to in-plane pulsating forces. The dynamic stability analysis of delaminated spherical shell structures subjected to in-plane pulsating forces is carried out based on the higher-order shell theory of Sanders. In the finite element (FE) formulation, the seven degrees of freedom per each node are used with transformations in order to fit the displacement continuity conditions at the delamination region. The boundaries of the instability regions are determined using the method proposed by Bolotin.

**Aim and Scope of present study:**

The present study deals with the effect of delamination on dynamic characteristic of composites.

The various modules are:

- Vibration of delaminated composite shells
- Buckling of delaminated composite shells
- Dynamic stability of delaminated plates and shells

# CHAPTER 3

# MATHEMATICAL FORMULATION

## The Basic Problems

This chapter involves the finite element mathematical formulation for vibration, static and dynamic stability analysis of the plate and shell structures of various geometry with/without delamination. The basic configuration of the problem considered here is a doubly curved panel with mid plane single delamination subjected to in plane periodic load. The boundary conditions are incorporated in the most general manner.

## 1.1. Proposed Analysis

The governing equations for the dynamic stability of the delaminated composite plates and shell are derived on the basis of first order shear deformation theory .The element stiffness, geometric stiffness and mass matrices are derived on the basis of principle of minimum potential energy and Lagrange's equation.

**Governing equation for analysis:-**

Equation for free vibration is, $$([\boldsymbol{K}] - \boldsymbol{\omega}^2 [\boldsymbol{M}])\{\emptyset\} = \{\mathbf{0}\}$$

Where $[K]\ and\ [M]$ are the global stiffness and global mass matrices, $\omega$ is the natural frequency and $\emptyset$ is the corresponding eigenvectors i.e. mode shape.

Equation for buckling analysis is, $$([\boldsymbol{K}] - \boldsymbol{P}[\boldsymbol{K_g}])\{\emptyset\} = \{\mathbf{0}\}$$

Where $[K]$ and $[K_g]$ are the bending stiffness matrix and geometric stiffness matrix. The Eigen values of the above equation gives the buckling loads for different modes. The lowest value of buckling load (P) is termed as critical buckling load $(P_{cr})$of the structure.

Equation for dynamic stability analysis in line with [Radu and Chattopadhyay (2000) ],

$$\boldsymbol{K + (\alpha_0 \pm 0.5\alpha_1)P_{cr}K_G - 0.25M\theta^2 = 0}$$ Where M, K and $K_G$ are the mass, the stiffness and the geometric matrices. $\theta$ Represent the frequency, $\alpha_0$ and $\alpha_1$ are static and dynamic parameters taking values from 0 to 1.

**FINITE ELEMENT ANALYSIS**

A laminated doubly curved shell panel of length *a*, width *b* and thickness *h* consisting of *n* arbitrary number of anisotropic layers is considered as shown in Figure 1. The layer details of the laminate are shown in Figure 2. The displacement field is related to mid-plane displacements and rotations as

$$u(x,y,z,t) = u^0(x,y,z,t) + z\,\theta_x\,(x,y,t),$$

$$v(x,y,z,t) = v^0(x,y,z,t) + z\,\theta_y\,(x,y,t),$$

$$w(x,y,z,t) = w^0(x,y,z,t)\,,$$

Where *u*, *v* and *w* are displacements in *x*, *y* and *z* directions, respectively, and the superscript

($^0$) corresponds to the mid-plane values. Here, $\theta_x$ and $\theta_y$ denote the rotations of the cross-sections perpendicular to the *y*- and *x*-axis respectively. Using Sander's first approximation theory for thin shells, the generalized strains in terms of mid-plane strains and curvatures are expressed as

$$\{ \epsilon_{xx} \ \epsilon_{yy} \ \gamma_{xy} \ \gamma_{xz} \ \gamma_{yz} \}^T = \{ \epsilon^0_{xx} \ \epsilon^0_{yy} \ \gamma^0_{xy} \ \gamma^0_{xz} \ \gamma^0_{yz} \}^T + \{ k_{xx} \ k_{yy} \ k_{xy} \ k_{xz} \ k_{yz} \}^T ,$$

Where,

$$\begin{Bmatrix} \epsilon^0_{xx} \\ \epsilon^0_{yy} \\ \gamma^0_{xy} \\ \gamma^0_{xz} \\ \gamma^0_{yz} \end{Bmatrix} = \begin{Bmatrix} \frac{\partial u^0}{\partial x} + \frac{\omega}{R_x} \\ \frac{\partial v^0}{\partial y} + \frac{\omega}{R_y} \\ \frac{\partial u^0}{\partial y} + \frac{\partial v^0}{\partial x} + \frac{2\omega}{R_{xy}} \\ \theta_x + \frac{\partial \omega}{\partial x} \\ \theta_y + \frac{\partial \omega}{\partial y} \end{Bmatrix}$$

And

$$\begin{Bmatrix} k_{xx} \\ k_{yy} \\ k_{xy} \\ k_{xz} \\ k_{yz} \end{Bmatrix} = \begin{Bmatrix} \frac{\partial \theta_x}{\partial x} \\ \frac{\partial \theta_y}{\partial y} \\ \frac{\partial \theta_x}{\partial x} + \frac{\partial \theta_y}{\partial y} \\ 0 \\ 0 \end{Bmatrix}$$

And $R_x$ , $R_y$ and $R_{xy}$ are the three radii of curvature of the shell element. The entire dynamic

Equations of equilibrium reduce to that for the plate, when the values of $R_x$, $R_y$, and $R_{xy}$ become $\infty$. The five degrees of freedom considered at each node of the element are $u^0$, $v^0$, $w$, $\theta x$ and $\theta y$. By using the eight-nodded element shape functions, the element displacements are expressed in terms of their nodal values given by

$$u^0 = \sum_{i=1}^{\infty} N_i \, u_i^0 \quad , \quad v^0 = \sum_{i=1}^{\infty} N_i \, v_i^0 \quad , \quad \omega^0 = \sum_{i=1}^{\infty} N_i \, \omega_i$$

$$\theta_x = \sum_{i=1}^{\infty} N_i \, \theta_{xi} \qquad \theta_y = \sum_{i=1}^{\infty} N_i \, \theta_{yi}$$

Where $N_i$ '*s* are the shape functions used to interpolate the generalized displacements $u_i^0$, $v_i^0$.

$\omega_i$ , $\theta_{xi}$and $\theta_{yi}$ at node *i* within an element.

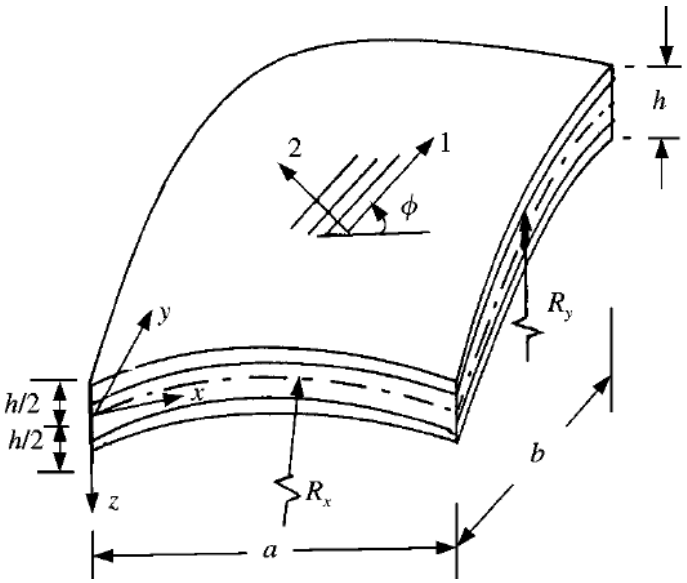


Figure 1. laminated doubly curved composite shell axes

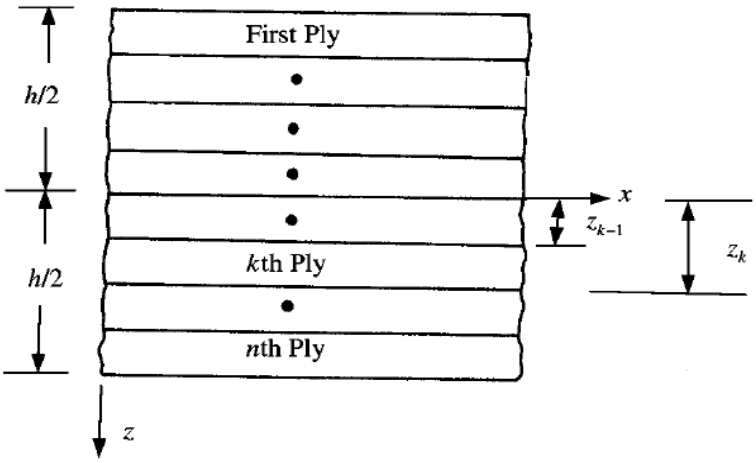


f igure 2. Layer details of shell panel.

The stress resultants are related to the mid-plane strains and curvatures for a general laminated shell element as

$$\begin{Bmatrix} N_x \\ N_y \\ N_{xy} \\ M_x \\ M_y \\ M_{xy} \\ Q_y \\ Q_x \end{Bmatrix} = \begin{bmatrix} A_{11} & A_{12} & A_{16} & B_{11} & B_{12} & B_{16} & 0 & 0 \\ A_{12} & A_{22} & A_{26} & B_{12} & B_{22} & B_{26} & 0 & 0 \\ A_{16} & A_{26} & A_{66} & B_{16} & B_{26} & B_{66} & 0 & 0 \\ B_{11} & B_{12} & B_{16} & D_{11} & D_{12} & D_{16} & 0 & 0 \\ B_{12} & B_{22} & B_{26} & D_{12} & D_{22} & D_{26} & 0 & 0 \\ B_{16} & B_{26} & B_{66} & D_{16} & D_{26} & D_{66} & 0 & 0 \\ 0 & 0 & 0 & 0 & 0 & 0 & A_{44} & A_{45} \\ 0 & 0 & 0 & 0 & 0 & 0 & A_{45} & A_{55} \end{bmatrix} \begin{Bmatrix} \varepsilon^0_{xx} \\ \varepsilon^0_{yy} \\ \gamma^0_{xy} \\ K_{xx} \\ K_{yy} \\ K_{xy} \\ \gamma^0_{yz} \\ \gamma^0_{xz} \end{Bmatrix}$$

Where $N_x$, $N_y$ and $N_{xy}$ are in-plane stress resultants,$M_x$ , $M_y$ and $M_{xy}$ are moment resultants and $Q_x$, $Q_x$ are transverse shear stress resultants. The extensional, bending-stretching and bending stiffness's of the laminate are expressed in the usual form as

$$(\text{Aij, Bij, Dij}) = \sum_{k=1}^{n} \int_{z_{k-1}}^{z_k} \left(\overline{Q_{ij}}\right)_k (1, z, z^2)\, dz, \qquad i, j = 1, 2, 6.$$

Similarly, the shear stiffness is expressed as

$$(A_{ij}) = \sum_{k=1}^{n} \int_{z_{k-1}}^{z_k} \alpha(\overline{Q_{ij}})_k \, dz, \qquad i, j = 4, 5.$$

$\alpha$ is the shear correction factor which is derived from the Timoshenko beam concept by applying the energy principle is assumed as 5/6. It accounts for the non-uniform distribution of transverse shear strain across the thickness of the laminate.

$(\overline{Q_{ij}})k$ in equations (6) and (7) are the off-axis stiffness values defined as

$$(\bar{Q}_{ij})_k = \begin{bmatrix} m^2 & n^2 & -2mn \\ n^2 & m^2 & 2mn \\ mn & -mn & m^2 - n^2 \end{bmatrix} (Q_{ij})_k \begin{bmatrix} m^2 & n^2 & mn \\ n^2 & m^2 & -mn \\ -2mn & 2mn & m^2 - n^2 \end{bmatrix}, \qquad i, j = 1, 2, 6.$$

$$(\bar{Q}_{ij})_k = \begin{bmatrix} m & -n \\ n & m \end{bmatrix} (Q_{ij})_k \begin{bmatrix} m & n \\ -n & m \end{bmatrix}, \qquad i, j = 4, 5.$$

Where, $m=\cos\theta$ , $n=\sin\theta$

$(Q_{ij})_k$ are calculated in the conventional manner from the values of elastic and shear moduli and the Poisson ratio values.

$Q_{11} = E_1/(1-\upsilon_{12}\upsilon_{21})$ , $Q_{12} = \upsilon_{12}E_2/(1-\upsilon_{12}\upsilon_{21})$, $Q_{21} = \upsilon_{12}\, E_2/(1-\upsilon_{12}\upsilon_{21})$ , $Q_{22} = E_2/(1-\upsilon_{12}\upsilon_{21})$

$Q_{66}= G_{12}$, $Q_{44}= G_{13}$, $Q_{55}= G_{23}$.

$E_{1,}$ $E_2$ = Young's moduli of a lamina along and across the fibres, respectively

$G_{12,}$ $G13_{,}$ $G_{23}$ = Shear moduli of a lamina with respect to 1,2 and 3 axes.

$\upsilon_{12}$ ,$\upsilon_{21}$ = Poisson's ratios.

The element stiffness matrix, $[K_e]$ is given by

$$[K_e] = \int_{-1}^{1}\int_{-1}^{1}[B]^T[D][B]J\,d\xi\,d\eta$$

Where [B] is stain-displacement matrix

[D] is the elasticity matrix

J is the Jacobean

Full integration (3x3) is used for bending stiffness, whereas reduced integration (2x2) is employed to evaluate transverse stiffness of the elements. A 2 point integration eliminates the shear locking in case of thin plates.

Similarly the consistent element mass matrix $[M_e]$ is expressed as

$$[M_e] = \int_{-1}^{1}\int_{-1}^{1}[N]^T[\rho][N]J\,d\xi\,d\eta$$

With [N], the shape function matrix and $[\rho]$, the inertia matrix.

The element load vector,$\{F_e\}$ is presented by

$$[M_e] = \int_{-1}^{1}\int_{-1}^{1} [N]^T \{q\} J d\xi d\eta$$

Where {q} is the intensity of external transverse uniform loading.

The shape functions $N_i$ are defined as

$N_i = (1+\xi\xi_i)(1+\eta\eta_i)(\xi\xi_i + \eta\eta_i - 1)/4$ i=1to4

$N_i = (1-\xi^2)(1+\eta\eta_i)/2$ i=5,7

$N_i = (1+\xi\xi_i)(1-\eta^2)/2$ i=6,8

Where $\xi$ and $\eta$ are the local natural coordinates of the element and $\xi_i$ and $\eta_i$ are the values at $i^{th}$ mode. The derivatives of the shape function $N_i$ with respect to x,y are expressed in term of their derivatives with respect to $\xi$ and $\eta$ by the following relationship

$$\begin{bmatrix} N_{i,x} \\ N_{i,y} \end{bmatrix} = [J]^{-1} \begin{bmatrix} N_{i,\xi} \\ N_{i,\eta} \end{bmatrix}$$

Where $[J] = \begin{bmatrix} \frac{\partial x}{\partial \xi} & \frac{\partial y}{\partial \xi} \\ \frac{\partial x}{\partial \eta} & \frac{\partial y}{\partial \eta} \end{bmatrix}$

**Strain displacement Relations**

Green-Lagrange's strain displacement is used throughout the structural analysis. The linear part of the strain is used to derive the elastic stiffness matrix and non-linear part of the strain is used to derive the geometrical stiffness matrix.

$\{\varepsilon\} = \{\varepsilon_l\} + \{\varepsilon_{nl}\}$

The linear strains are defined as

$$\epsilon_{xl} = \frac{\partial u}{\partial x} + \frac{w}{R_x} + Zk_x$$

$$\epsilon_{yl} = \frac{\partial u}{\partial y} + \frac{w}{R_y} + Zk_y$$

$$\gamma_{xyl} = \frac{\partial u}{\partial y} + \frac{\partial v}{\partial x} + \frac{2w}{Rx_y} + Zk_{xy}$$

$$\gamma_{xz} = \frac{\partial u}{\partial z} + \frac{\partial w}{\partial x} - C_1\frac{u}{R_x} - C_1\frac{v}{R_{xy}}$$

$$\gamma_{yz} = \frac{\partial w}{\partial y} + \frac{\partial v}{\partial z} - \frac{v}{R_y} - C_1\frac{u}{R_{xy}}$$

Where the bending strains $k_j$ are expressed as

$$K_x = \frac{\partial \theta_x}{\partial x},$$

$$K_y = \frac{\partial \theta_y}{\partial y}$$

$$K_{xy} = \frac{\partial \theta_x}{\partial y} - \frac{\partial \theta_y}{\partial x} + \frac{1}{2}C_2\left(\frac{1}{R_y} - \frac{1}{R_x}\right)\left(\frac{\partial v}{\partial x} - \frac{\partial u}{\partial y}\right)$$

And $C_1$ and $C_2$ are tracers by which the analysis can be reduced to that of shear deformable love's first approximations and Donnell's theories.

Assuming that *w* does not vary with *z*, the non-linear strains of the shell are expressed as

$\varepsilon_{xnl} = [ (u,_x + w/R_x)^2 + v_{,x}^2 + (w,_x - u/R_x)^2]/2,$

$\varepsilon_{ynl} = [ (v,_y + w/R_y)^2 + u_{,y}^2 + (w,_y - v/R_y)^2]/2,$

$\gamma_{xynl} = [ (u,_x + w/R_x)u,_y + v,_x(v,_y + w/R_y) + (w,_x - u/R_x)\ (w,_y - v/R_y)],$

$\gamma_{xznl}$ = [ $(u,_x + w/R_x)u,_z + v,_x v,_z + (w,_x - u/R_x)\, w,_z$],

$\gamma_{yznl}$ = [ $(u,_y + w/R_y)u,_z + v,_y v,_z + (w,_y - u/R_y)\, w,_z$],

The linear strain can be described in term of displacements as

$$\{\epsilon\} = [B]\ \{de\}$$

Where $\{de\} = [u_1 \quad v_1 \quad w_1 \quad \theta_{x1} \quad \theta_{y1} \quad u_2 \quad v_2 \cdots\cdots\cdots u_8 \quad v_8 \quad w_8 \quad \theta_{x8} \quad \theta_{y8}]^T$

$$[B] = [\,[B_1] \quad [B_2] \cdots\cdots [B_7] \quad [B_8]\,]$$

$$[B_i] = \begin{bmatrix} \frac{\partial Ni}{\partial x} & 0 & \frac{N_i}{R_x} & 0 & 0 \\ 0 & \frac{\partial Ni}{\partial y} & \frac{N_i}{R_y} & 0 & 0 \\ \frac{\partial Ni}{\partial y} & \frac{\partial Ni}{\partial x} & 0 & 0 & 0 \\ 0 & 0 & 0 & \frac{\partial Ni}{\partial x} & 0 \\ 0 & 0 & 0 & 0 & \frac{\partial Ni}{\partial y} \\ 0 & 0 & 0 & \frac{\partial Ni}{\partial y} & \frac{\partial Ni}{\partial x} \\ 0 & 0 & \frac{\partial Ni}{\partial x} & Ni & 0 \\ 0 & 0 & \frac{\partial Ni}{\partial y} & 0 & Ni \end{bmatrix}$$

Generalised element mass matrix or consistent mass matrix:-

$$[M_e] = \int_{-1}^{1}\int_{-1}^{1}[N]^T[\rho][N]Jdxdy$$

Where the shape function matrix

$$[N] = \begin{bmatrix} Ni & 0 & 0 & 0 & 0 \\ 0 & Ni & 0 & 0 & 0 \\ 0 & 0 & Ni & 0 & 0 \\ 0 & 0 & 0 & Ni & 0 \\ 0 & 0 & 0 & 0 & Ni \end{bmatrix}$$

$$[P] = \begin{bmatrix} P_1 & 0 & 0 & P_2 & 0 \\ 0 & P_1 & 0 & 0 & P_2 \\ 0 & 0 & P_1 & 0 & 0 \\ P_2 & 0 & 0 & P_3 & 0 \\ 0 & P_2 & 0 & 0 & P_3 \end{bmatrix}$$

Where,

$$(P_1, \quad P_2, \quad P_3) = \sum_{k=1}^{n} \int_{z_{k-1}}^{z_k} (\rho)_k \, (1, z, z^2) \, dz,$$

The element mass matrix can be expressed in local natural co-ordinate of the element as.

$$[M_e] = \int_{-1}^{1} \int_{-1}^{1} [N]^T [\rho] [N] J d\xi d\eta$$

**Geometric Stiffness Matrix:**

The element geometric stiffness matrix is derived using the non-linear in-plane Green's strains. The strain energy due to initial stresses is

$$U_2 = \int_v [\sigma^0]^T \{\varepsilon_{nl}\} dV$$

Using non-linear strains, the strain energy can be written in matrix form as

$$U_2 = \frac{1}{2} \int_v [f]^T [S] [f] dV$$

$$\{f\} = \left[\frac{\partial u}{\partial x}, \frac{\partial u}{\partial y}, \frac{\partial v}{\partial x}, \frac{\partial v}{\partial y}, \frac{\partial w}{\partial x}, \frac{\partial w}{\partial y}, \frac{\partial \theta_x}{\partial x}, \frac{\partial \theta_x}{\partial y}, \frac{\partial \theta_y}{\partial x}, \frac{\partial \theta_y}{\partial y}\right]^T$$

$$[S] = \begin{bmatrix} s & 0 & 0 & 0 & 0 \\ 0 & s & 0 & 0 & 0 \\ 0 & 0 & s & 0 & 0 \\ 0 & 0 & 0 & s & 0 \\ 0 & 0 & 0 & 0 & s \end{bmatrix}$$

$$[s] = \begin{bmatrix} \sigma_x & \tau_{xy} \\ \tau_{xy} & \sigma_y \end{bmatrix} = \frac{1}{h}\begin{bmatrix} N_x & N_{xy} \\ N_{xy} & N_y \end{bmatrix}$$

The in-plane stress resultants $N_x$ , $N_y$, $N_{xy}$ at each gauss point are obtained by applying uniaxial stress in x-direction and the geometric stiffness matrix is formed for these stress resultants.

$$[f] = [G][\delta_e]$$

The strain energy becomes

$$U_2 = \frac{1}{2}\int \{\delta_e\}^T [G]^T [S][G]\{\delta_e\} dV = \frac{1}{2}\{\delta_e\}^T [K_g]\{\delta_e\}$$

Where element geometric stiffness matrix $[K_g]_e = \int\int\int [G]^T [S][G] dV$

$$[G] = \begin{bmatrix} N_{i,x} & 0 & 0 & 0 & 0 \\ N_{i,y} & 0 & 0 & 0 & 0 \\ 0 & N_{i,x} & 0 & 0 & 0 \\ 0 & N_{i,y} & 0 & 0 & 0 \\ -N_i/R_x & 0 & N_{i,x} & 0 & 0 \\ 0 & -N_i/R_y & N_{i,y} & 0 & 0 \\ 0 & 0 & 0 & N_{i,x} & 0 \\ 0 & 0 & 0 & N_{i,y} & 0 \\ 0 & 0 & 0 & 0 & N_{i,x} \\ 0 & 0 & 0 & 0 & N_{i,y} \end{bmatrix}$$

**Multiple delamination modelling**

Considering a typical composite laminate having p number of delamination is considered.

$$u_t = u_t^0 + (Z - Z_t^0)\theta_x \, , v_t = v_t^0 + (Z - Z_t^0)\theta_y \qquad (1)$$

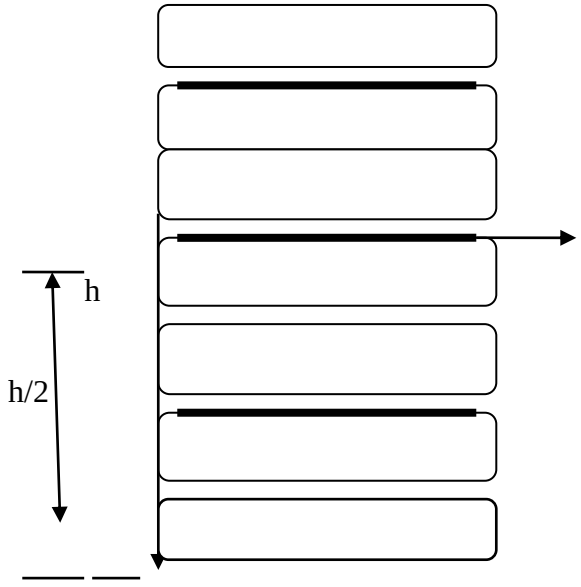


**Figure 3:** Multiple delamination model

Where $u_t^0$, $v_t^0$ are the mid-plane displacement of the $t^{th}$ sub laminate and $z_t^0$, the distance between the mid-plane of the original laminate and the mid-plane of the $t^{th}$ sub laminate. The strain component of any layer of a sub laminate are found from eqn (2) in the form of

$$\begin{Bmatrix} \epsilon_{xx} \\ \epsilon_{yy} \\ \gamma_{xy} \end{Bmatrix} = \begin{Bmatrix} \epsilon_{xx}^0 \\ \epsilon_{yy}^0 \\ \gamma_{xy}^0 \end{Bmatrix} + (Z - Z_t^0) \begin{Bmatrix} k_{xx} \\ k_{yy} \\ k_{xy} \end{Bmatrix} \qquad (2)$$

In the order to satisfy the compatibility condition at the delamination's boundary, it is assumed that transverse displacements and rotations at a common node for all the three sub laminates including the original one are identical. Applying this multipoint constraint condition,the midpoint displacements of any sub laminate t can be generalized as

$$u_t^0 = u^0 + Z_t^0\theta_x \,,\; v_t^0 = v^0 + Z_t^0\theta_y \qquad (3)$$

The mid plane strain components of the $t^{th}$ sub laminate are derived from it as

$$\begin{Bmatrix} \epsilon_{xx}^0 \\ \epsilon_{yy}^0 \\ \gamma_{xy} \end{Bmatrix} = \begin{bmatrix} \epsilon_{xx}^0 \\ \epsilon_{yy}^0 \\ \gamma_{xy}^0 \end{bmatrix} + Z_t^0 \begin{bmatrix} k_{xx} \\ k_{yy} \\ k_{xy} \end{bmatrix} \qquad (4)$$

Substituted $eq^n(4)$ into $eq^n(2)$,then we get strain components at any layer within a sub laminate. For any lamina of the $t^{th}$ sub laminate, the in-plane and shear stresses are fined from the relations

$$\begin{Bmatrix} \sigma_{xx} \\ \sigma_{yy} \\ \tau_{xy} \end{Bmatrix} = \begin{bmatrix} \overline{Q_{11}} & \overline{Q_{12}} & \overline{Q_{16}} \\ \overline{Q_{21}} & \overline{Q_{22}} & \overline{Q_{26}} \\ \overline{Q_{16}} & \overline{Q_{26}} & \overline{Q_{66}} \end{bmatrix} \begin{Bmatrix} \epsilon_{xx} \\ \epsilon_{yy} \\ \gamma_{xy} \end{Bmatrix}_t$$

$$\begin{Bmatrix} \tau_{xz} \\ \tau_{yz} \end{Bmatrix} = \begin{bmatrix} \overline{Q_{44}} & \overline{Q_{45}} \\ \overline{Q_{45}} & \overline{Q_{55}} \end{bmatrix} \begin{Bmatrix} \gamma_{xz} \\ \gamma_{yz} \end{Bmatrix}_t$$

Integrating these stresses over the thickness of the sub laminate, the stress and moment resultants of the sub laminate are desired which lend to the elasticity matrix of the $t^{th}$ sub laminate is the form

$$[D]_t = \begin{bmatrix} A_{ij} & Z_t^0 A_{ij} + B_{ij} & 0 \\ B_{ij} & Z_t^0 B_{ij} + D_{ij} & 0 \\ 0 & 0 & S_{ij} \end{bmatrix}$$

Where $[A_{ij}]_t = \int_{-\frac{h_t}{2}+Z_t^0}^{\frac{h_t}{2}+Z_t^0} [\bar{Q}_{ij}] dz$

$$[B_{ij}]_t = \int_{-\frac{h_t}{2}+Z_t^0}^{\frac{h_t}{2}+Z_t^0} [\bar{Q}_{ij}](Z - Z_t^0) dz$$

$$[D_{ij}]_t = \int_{-\frac{h_t}{2}+Z_t^0}^{\frac{h_t}{2}+Z_t^0} [\bar{Q}_{ij}](Z - Z_t^0)^2 dz \text{ , i,j=1,2,6}$$

$$[S_{ij}]_t = \int_{-\frac{h_t}{2}+Z_t^0}^{\frac{h_t}{2}+Z_t^0} [\bar{Q}_{ij}] dz \text{ , i,j=4,5}$$

Here $h_t$ is the thickness of the $t^{th}$ sub laminate.

**Analysis Method:-**

The finite element formulation is developed for the dynamic analysis of laminated composite shells with delamination using the first order shear deformation theory. An eight-nodded continuous doubly curved isoparametric element is employed in the present analysis with five degrees of freedom viz. u, v, w, $\theta x$, *and* $\theta y$ at each node.

The eigenvalue equation for the free vibration analysis of laminated composite plate and shell can be expressed as

$([K] - \omega^2 [M])\{\emptyset\} = \{0\}$, Where $[K]$ *and* $[M]$ the global stiffness and global mass matrices are, $\omega$ is the natural frequency and $\emptyset$ is the corresponding eigenvectors i.e. mode shape.

The eigenvalue equation for the stability analysis of laminated composite plate and shell can be expressed as

$$([K] - P[K_g])\{\emptyset\} = \{0\}$$

Where $[K]$ and $[K_g]$ are the bending stiffness matrix and geometric stiffness matrix. The Eigen values of the above equation gives the buckling loads for different modes. The lowest value of buckling load (P) is termed as critical buckling load $(P_{cr})$ of the structure.

The eigenvalue equation for the dynamic stability analysis of laminated composite plate and shell can be expressed as

$$K + (\alpha_0 \pm 0.5\alpha_1)P_{cr}K_G - 0.25M\theta^2 = 0$$ Where M, K and $K_G$ are the mass, the stiffness and the geometric matrices. $\theta$ Represent the frequency, $\alpha_0$ and $\alpha_1$ are static and dynamic parameters taking values from 0 to 1.

**Computer Program**:

A computer program based on finite element formulation developed in MATLAB 7.8.0. The element bending stiffness, geometric stiffness and mass matrices are derived by using functions. The program consists of sub function called inside the program. The sub function performs specific work at different levels of analysis. In the beginning of the program, dimensions of the plates and shells, and material properties of plates and shells defined by appropriate symbol. In the program several function used such as **assmbl** for assembling the stiffness, geometric stiffness and mass matrices. **Compo** function is used for finding the constituent matrices. **Gestiff** is used for finding geometric stiffness, **stiff** is used for finding bending stiffness, **massfsdt** is used for mass matrices, **and gener** is used for generalization of bending stiffness, geometric stiffness and mass matrices. For delamination, **delamcompo** function is used and also used two functions **top** and **bottom** for finding mid plane delamination effect. **Shaped** is used for finding out the shape function and **ndarr** is for boundary condition.

# CHAPTER 4

# RESULTS AND DISCUSSIONS

## Introduction:

Recently composite plates and shells as a structural element are widely using in aerospace, civil, mechanical and other engineering structures and playing a important role in such kind of industries.

In this chapter, the result of vibration, buckling and dynamic stability of plate and shell structures with and without delamination is presented by using above FEM formulation. The instability regions are determined for composite plates and shell with and without delamination and the results are presented for different delamination lengths and percentage.

The study is aimed upon the following studies.

- Comparison with previous studies
- Numerical Results

**Boundary conditions:**

Numerical results are presented for delaminated composite plates/shells with different combination of boundary conditions. Shells of various geometry such as spherical ($R_y/R_x$=1) and cylindrical ($R_y/R_x$=0) are studied.

Further descriptions of boundary conditions are as follows:

I. Simply supported boundary

v=w=$\theta_y$=0 at x=0, a and u=w=$\theta_x$=0 at y=0, b

II. Clamped boundary

u=v=w=$\theta_x$=$\theta_y$= 0 at x=0, a and y=0, b

III. Free edges

No restraint

**Non-dimensionalisation of Parameters:**

Following are the non-dimensional parameter using for vibration, buckling and excitation frequency of dynamic stability analysis with the reference Bert, C.W. and Birman, V. (1988).

**Table 1.1** Non-dimensional parameters of composite plates/shells

| No | parameter | Composite plates/ shells |
|---|---|---|
| 1 | Frequency of vibration ($\omega$) | $\varpi a^2 \sqrt{\rho/h^2}\, E_2$ |
| 2 | Buckling load ($\lambda$) | $N_x \frac{a^2}{E_2\, h^3}$ |
| 3 | Frequency of excitation ($\Omega$) | $\bar{\Omega} a^2 \sqrt{\rho/h^2}\, E_2$ |

Where $\varpi$ and $\bar{\Omega}$ are in radian.

## Comparison with previous studies:

The vibration, buckling of plates/shells and dynamic stability results of plates based on present formulation are compared with that of existing literature.

**Vibration of composite plates and shells**

The result on free vibration of cross-ply delaminated plates and shell are compared with result by parhi *et al* (2002) using first order shear deformation theory. The program of the

finite element formulation developed in MATLAB 7.8.0 and validated by comparing the author's results with those available in the existing literature. For this free vibration analysis, the boundary conditions used in present study is simply supported and composite (0/90/0/90) spherical and cylindrical shell and plates with delamination is carried out with the following geometric and material properties:

Present result of natural frequencies (Hz) for mid-plane delaminated plates, cylindrical and spherical shells are shown in table 1 along with the result of Parhi (2002) et al.

.Geometry and material properties: a=b=0.5m, a/h=100, R/a=5 and R/a=10, $\vartheta_{12}$=0.25, $\rho = 1600kg/m^3$,

$E_{11} = 172.5GPa.\ E_{22} = 6.9GPa,\ G_{12} = G_{13} = 3.45GPa,\ G_{23} = 1.38GPa$ .

**Table1.2**. Natural frequencies (Hz) for mid-plane delaminated simply supported composite spherical, cylindrical shells and plates with different delamination.

| % delamination | Stacking sequence | Spherical shell (R/a=10) | | Cylindrical shell (R/a=10) | | Plate (R/a=∞) | |
|---|---|---|---|---|---|---|---|
| | | present | Parhi et al(2002) | present | Parhi et al(2002) | present | Parhi et al(2002) |
| 0 | $(0/90)_2$ | 129.1353 | 129.20 | 103.0197 | 103.03 | 92.7162 | 92.72 |
| 25 | $(0/90)_2$ | 104.5625 | 104.59 | 69.5945 | 69.60 | 52.9273 | 52.93 |
| 56.25 | $(0/90)_2$ | 98.3438 | 98.36 | 59.9258 | 59.88 | 39.5013 | 39.50 |

**Table1.3**. Natural frequencies (Hz) for mid-plane delaminated simply supported composite spherical and cylindrical shells with different delamination.

| % delamination | Stacking sequence | Spherical shell (R/a=5) | | Cylindrical shell (R/a=5) | |
|---|---|---|---|---|---|
| | | present | Parhi et al (2002) | present | Parhi et al (2002) |
| 0 | $(0/90)_2$ | 201.8568 | 202.02 | 128.9892 | 129.04 |
| 25 | $(0/90)_2$ | 187.4469 | 187.51 | 104.5625 | 104.56 |
| 56.25 | $(0/90)_2$ | 183.9246 | 183.96 | 98.2757 | 98.24 |

## Buckling of composite plates:

The present formulation is validated for buckling of cross-ply composite plates with and without delamination with result by Librescu et al (1989), Sciuva and Carrera (1990), Sahu (2001) and Radu and chattopadhyay (2002).

**Table 2.1**: Comparison of non-dimensional buckling loads of a square simply supported doubly curved panel with (0/90) lamination.

a/b=1, a/h=10, $E_{11}=40E_{22}$, $G_{12}=G_{13}=0.6E_{22}$, $G_{23}=0.5E_{22}$, $\vartheta_{12}=\vartheta_{23}=0.25$

$$\bar{N}_x = N_x \frac{a^2}{E_2 h^3}$$

Taken value, a=0.5, b=0.5, t=0.05, $E_{11}=160$GPa, $E_{22}=4$GPa, $G_{12}=G_{13}=2.4$GPa, $G_{23}=2$GPa.

Spherical shell (0/90)

| Curvature | Present Work | Sahu and Dutta(2001) | Librescu et al (1989) |
|---|---|---|---|
| $R_x/a=5$, $R_y/a=5$ | 12.018 | 11.920 | 12.214 |
| $R_x/a=10$, $R_y/a=5$ | 11.649 | 11.515 | 11.822 |
| $R_x/a=10$, $R_y/a=20$ | 11.245 | 11.250 | 11.479 |
| $R_x/a=20$, $R_y/a=20$ | 11.187 | 11.164 | 11.406 |
| Plate | 11.114 | 11.115 | 11.353 |

Numerical computation is carried out to determine the capability of the present delaminated doubly curved element to predict the buckling of laminated composite plates. The results obtained by this present formulation are compared with the analytical and finite element displacement approach results of Sciuva and Carrera (1990) and FEM result by Sahu and Dutta for 0% of delamination.

**Table 2.2:** Comparison of non-dimensional buckling loads of a square simply supported symmetric cross-ply cylindrical shell panels with [0/90/0/90/0] lamination for different length-to-thickness ratio (a/h). a/b=1, R/a=20, $E_{11}=40E_{22}$, $G_{12}=G_{13}=0.6E_{22}$, $G_{23}=0.5E_{22}$, $\vartheta_{12}=\vartheta_{23}=0.25$, $\bar{N}_x = N_x \frac{a^2}{E_2 h^3}$

Taken value, a=0.5, b=0.5, t=0.05, $E_{11}=160$GPa, $E_{22}=4$GPa, $G_{12}=G_{13}=2.4$GPa, $G_{23}=2$GPa.

Cylindrical Shell (0/90/0/90/0), $R_y=10$.

| a/h | Present Work | Sahu and Dutta (2001) | Sciuva and Carrera(1990) |
|---|---|---|---|
| 10 | 24.331 | 23.962 | 24.19 |
| 20 | 32.169 | 31.790 | 31.91 |
| 30 | 34.353 | 33.980 | 34.04 |
| 50 | 35.786 | 35.393 | 35.42 |
| 100 | 37.399 | 36.843 | 36.843 |

The results on buckling with different delamination length of cross-ply composite plates due to dynamic load is compared with results by Radu and Chattopadhyay (2002) using higher order shear deformation theory.

**Table 2.3** Comparison of critical buckling load for different mid plane delamination length of the rectangular plates using cantilever boundary condition.

$\rho = 1600kg/m^3$,

$E_{11} = 134.4GPa.\ E_{22} = 10.34GPa,\ G_{12} = G_{13} = 4.999GPa,\ G_{23} = 1.999GPa$ . a= 127mm, b=12.7mm, h=1.016mm, stacking sequence= (0/90/0/90/90/0/90/0).

| Delamination length (mm) | Critical buckling load (N) | |
|---|---|---|
| | Present work | Radu and Chattopadhyay (2002) |
| 0 | 16.3296 | 16.336 |
| 25.4 | 15.8292 | 16.068 |
| 50.8 | 14.9085 | 15.054 |

## Numerical Results:

Numerical validation of the governing equation of the composite plate and shell for vibration and buckling is performed by solving the corresponding free vibration equation and buckling equation eigenvalue problems. Finally, the dynamic stability phenomenon is investigated for effect of layers of ply, different degree of orthotropic, different static load factor, different length-thickness ratio and aspect ratio.

**Numerical results of vibration** are presented for simply supported square plate and shell having following Geometry and material properties: a=b=0.5m, a/h=100, R/a=5 and R/a=10, $\vartheta_{12}$=0.25, $\rho = 1600kg/m^3$,

$E_{11} = 172.5GPa.\ E_{22} = 6.9GPa,\ G_{12} = G_{13} = 3.45GPa,\ G_{23} = 1.38GPa$ .

Numerical results of natural frequency of composite spherical and cylindrical shell having different curvatures with 25% delamination for different no. Of layers with four sides simply supported boundary condition are presented in Table 3.1. Variation of natural frequency with no of layers of composite shell with 25% delamination is graphically presented in figure 4. It observed that, as number of layers increase for 2 to 16 the natural frequency also increases.

**Table3.1.** Natural frequencies (Hz) for 25% delaminated cross ply-$(0/90)_n$ simply supported composite spherical and cylindrical shells with different no. of layers.

| No. of layers | Spherical shell | | Cylindrical shell | |
|---|---|---|---|---|
| | (R/a=5) | (R/a=10) | (R/a=5) | (R/a=10) |
| 2 | 188.8401 | 107.0587 | 107.0618 | 73.3193 |
| 4 | 187.4469 | 104.5625 | 104.5625 | 69.5945 |
| 8 | 190.7261 | 110.4770 | 110.4207 | 78.2414 |
| 16 | 191.5230 | 111.8759 | 111.8008 | 80.2093 |

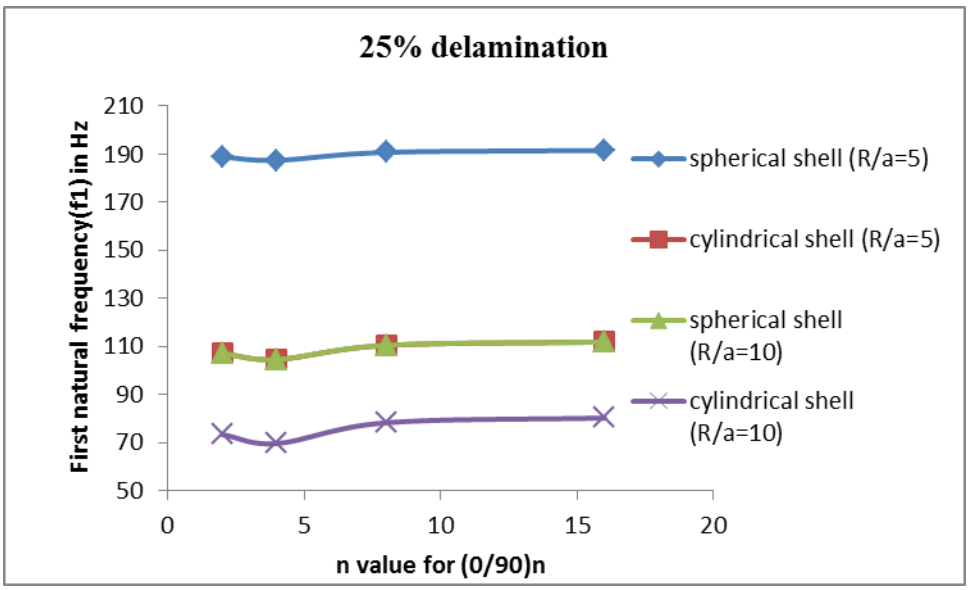


**Figure 4**: First natural frequency vs. no. of layer for simply supported composite shell with a single mid-plane delamination.

Natural frequency of composite spherical and cylindrical shell for different aspect ratio at 25% delamination is investigated in Table 3.2. The variation of natural frequency with different aspect ratio is graphically presented in fig 5. It observed that as aspect ratio increases the natural frequency decreases.

**Table3.2**. Natural frequencies (Hz) for 25% delaminated cross ply-$(0/90)_2$ simply supported composite spherical and cylindrical shells with different aspect ratio.

| a/b | Spherical shell<br>$R_x/a=5$, $R_y/b=5$ | Cylindrical shell<br>$R_x/a=\infty$, $R_y/b=5$ |
|---|---|---|
| 0.5 | 293.8187 | 220.6784 |
| 1 | 187.4469 | 104.5625 |
| 1.5 | 153.3563 | 71.5290 |
| 2 | 134.7433 | 56.4072 |

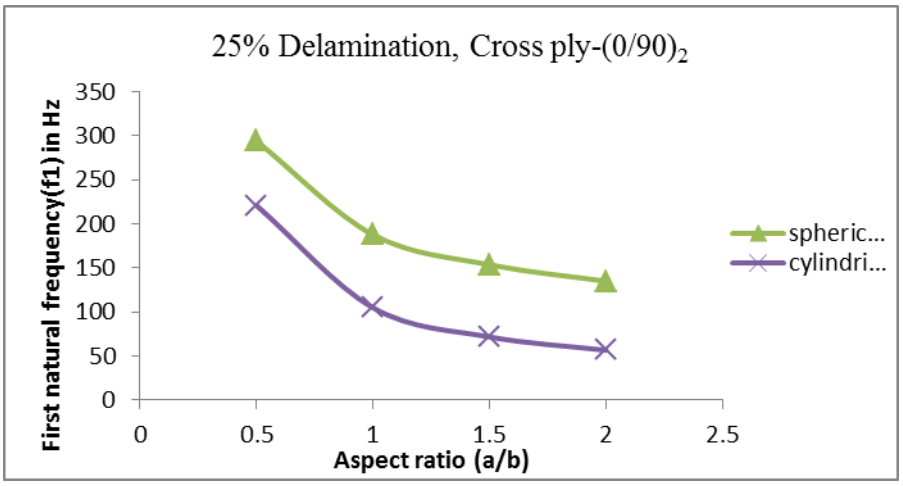


**Figure5**. First natural frequency vs. aspect ratio for simply supported composite shell with a single mid-plane delamination.

Natural frequency of delaminated composite cross-ply $(0/90)_2$ spherical and cylindrical shell for different side to thickness ratio is presented in table3.3. Variations of natural frequency with different % of delamination with different b/h ratio are presented in fig 6. It represent that as b/h ratio is increases, the natural frequency is also increases at 25 % of delaminated case.

**Table3.3**. Natural frequencies (Hz) for delaminated cross ply-$(0/90)_2$ simply supported composite spherical and cylindrical shells with different b/h ratio for R/a=5.

| % delamination | Spherical shell | | | Cylindrical shell | | |
|---|---|---|---|---|---|---|
| | b/h=100 | b/h=50 | b/h=25 | b/h=100 | b/h=50 | b/h=25 |
| 0 | 201.8568 | 256.4682 | 400.9718 | 128.9892 | 204.7105 | 371.4012 |
| 25 | 187.4469 | 208.1226 | 273.6824 | 104.5625 | 138.5553 | 226.2074 |
| 56.25 | 183.9246 | 195.9246 | 237.0790 | 98.2757 | 119.4906 | 179.8898 |

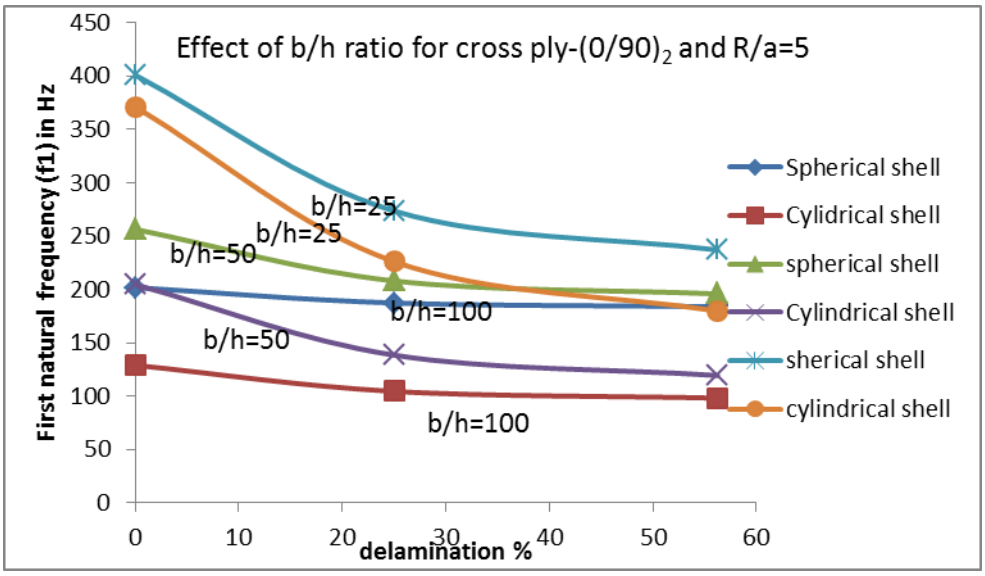


**Figure6**. First natural frequency vs. delamination % at different b/h ratio for simply supported composite shell with a single mid-plane delamination.

Table3.4 and fig 7 shows that the numerical result of natural frequency of spherical and cylindrical shell with different degree of orthotropic with different % of delamination. Fig 7 represent the natural frequency decreases with % delamination increases at each different degree of orthotropy.

**Table3.4**. Natural frequencies (Hz) for delaminated cross ply-$(0/90)_2$ simply supported composite spherical and cylindrical shells with different orthotropic ratio for R/a=5.

| $E_1/E_2$ | Spherical shell % delamination | | | Cylindrical shell % delamination | | |
|---|---|---|---|---|---|---|
| | 0 | 25 | 56.25 | 0 | 25 | 56.25 |
| 10 | 308.9156 | 238.2747 | 216.4470 | 271.7676 | 186.6011 | 157.7208 |
| 25 | 201.8568 | 187.4469 | 183.9246 | 128.9892 | 104.5625 | 98.2757 |
| 40 | 470.1998 | 300.8696 | 252.0983 | 445.2868 | 257.5297 | 197.9235 |

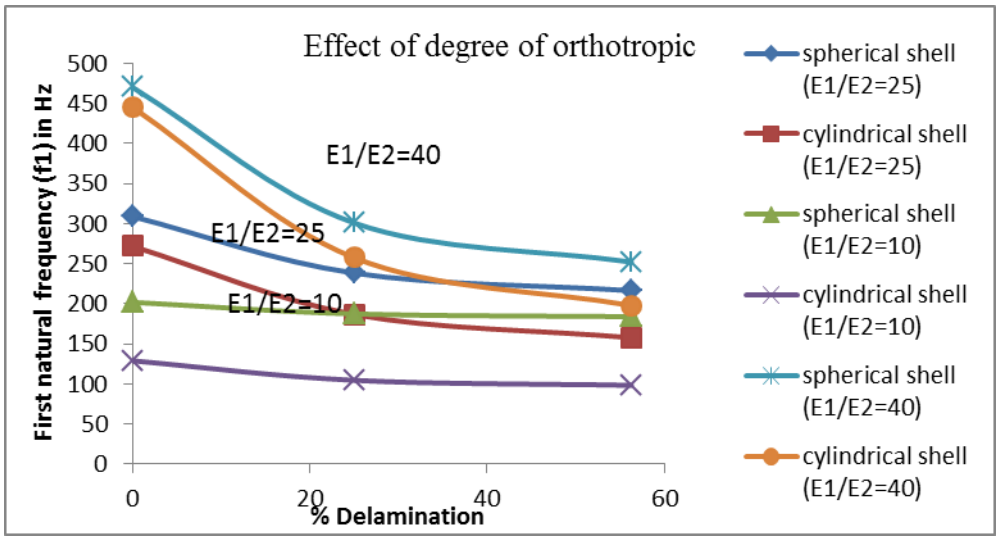


**Figure7**. First natural frequency vs. delamination % at different E1/E2 ratio for simply supported composite shell with a single mid-plane delamination.

**Numerical results of buckling** are presented for simply supported square plate and shell. The program of the finite element formulation developed in MATLAB 7.8.0 and validated by

comparing the author's results with those available in the existing literature. For this stability analysis, the boundary conditions used in present study is simply supported. And composite $(0/90)_n$ spherical and cylindrical shell and plates with and without delamination is carried out with the following geometric and material properties: a/b=1, a/h=10, $E_{11}=40E_{22}$, $G_{12}=G_{13}=0.6E_{22}$, $G_{23}=0.5E_{22}$, $\vartheta_{12}=\vartheta_{23}=0.25$.

Numerical results of non-dimensional buckling load with different no of layers for 0% delaminated composite plate and shell with different curvature are presented in table 4.1 ,Table 4.2 , and Table 4.3 . The variation of non-dimensional buckling load with different no of layers is presented in fig 8, fig 9, and fig 10. It observed that as no of layers increases the non-dimensional buckling load increases.

**Table 4.1:** Variation of non-dimensional buckling load with different no. of layers for 0% delaminated composite shell. $R_x/a=5$, $R_y/a=5$ cross-ply-$(0/90)_n$

| No. of layers | Spherical shell | Cylindrical shell | Plate |
|---|---|---|---|
| 3 | 22.0426 | 21.3819 | 21.2575 |
| 5 | 24.6990 | 23.9196 | 23.8427 |
| 7 | 25.7988 | 24.8905 | 24.8387 |
| 9 | 26.5486 | 25.4525 | 25.4205 |

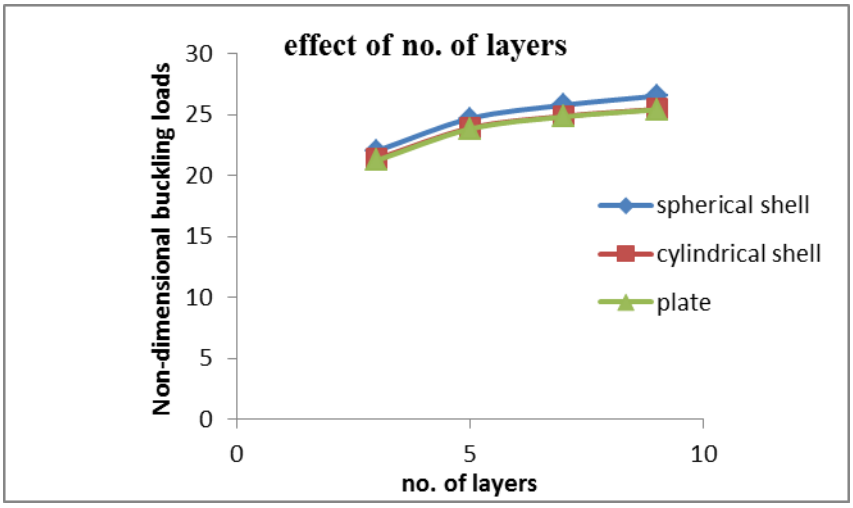


**Figure 8:** Variation of non-dimensional buckling load vs. no. of layers for simply supported composite shell. $R_x/a=5$, $R_y/a=5$, cross-ply-$(0/90)_n$

**Table 4.2:** Variation of non-dimensional buckling load with different no. of layers for 0% delaminated composite shell. $R_x/a=10$, $R_y/a=10$ cross-ply-$(0/90)_n$

| No. of layers | Spherical shell | Cylindrical shell | Plate |
|---|---|---|---|
| 3 | 21.4528 | 21.2887 | 21.2575 |
| 5 | 24.0540 | 23.8620 | 23.8427 |
| 7 | 25.0715 | 24.8516 | 24.8387 |
| 9 | 25.6833 | 25.4284 | 25.4205 |

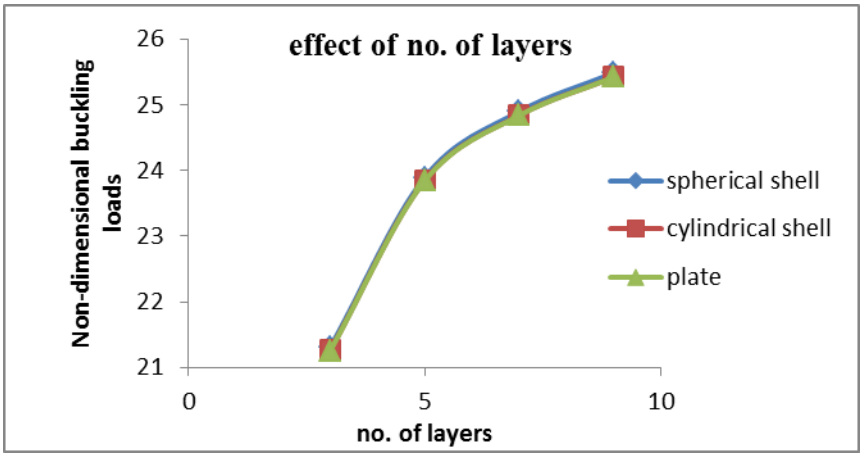


**Figure 9:** Variation of non-dimensional buckling load vs. no. of layers for simply supported composite shell. $R_x/a=10$ $R_y/a=10$, cross-ply-$(0/90)_n$

**Table 4.3:** Variation of non-dimensional buckling load with different no. of layers for 0% delaminated composite shell. $R_x/a=20$, $R_y/a=20$ cross-ply-$(0/90)_n$

| No. of layers | Spherical shell | Cylindrical shell | Plate |
|---|---|---|---|
| 3 | 21.3063 | 21.2633 | 21.2575 |
| 5 | 23.8954 | 23.8475 | 23.8427 |
| 7 | 24.8965 | 24.8419 | 24.8387 |
| 9 | 25.4854 | 25.4225 | 25.4205 |

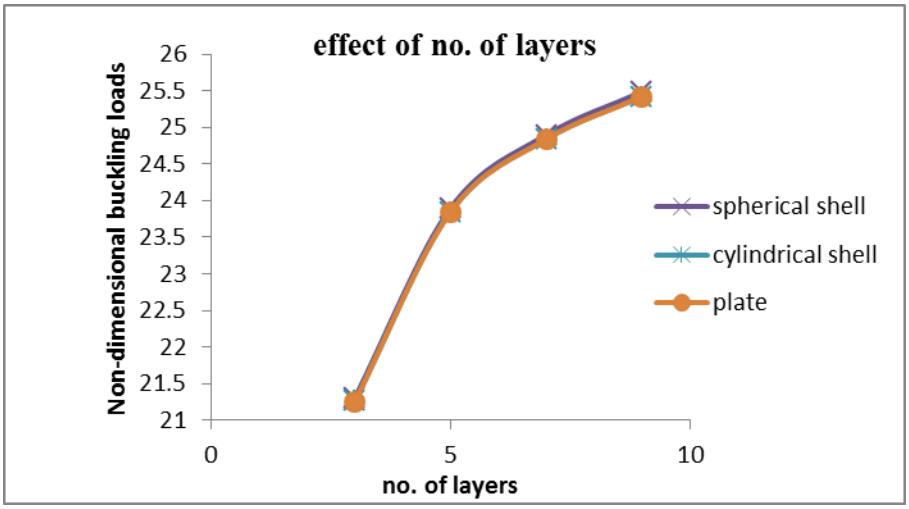


**Figure 10:** Variation of non-dimensional buckling load vs. no. of layers for simply supported composite shell. $R_x/a=20$, $R_y/a=20$, cross-ply-$(0/90)_n$.

Table 4.4 and Table 4.5 represent the numerical result of non-dimensional buckling load with different b/h ratio for 0% delamination of composite shell. The variation of non-dimensional buckling load with different b/h ratio is presented in fig 11 and fig 12. It investigated that as b/h ratio increases the non-dimensional buckling load increases.

**Table 4.4:** Variation of non-dimensional buckling load with different b/h ratio for 0% delaminated composite shell. $R_x/a=5$, $R_y/a=5$, $E_1=10E_2$, cross-ply-(0/90/0/90/0)

| b/h | Spherical shell | Cylindrical shell |
|---|---|---|
| 10 | 6.8671 | 6.6333 |
| 25 | 10.0591 | 9.0030 |
| 50 | 14.8080 | 10.5171 |

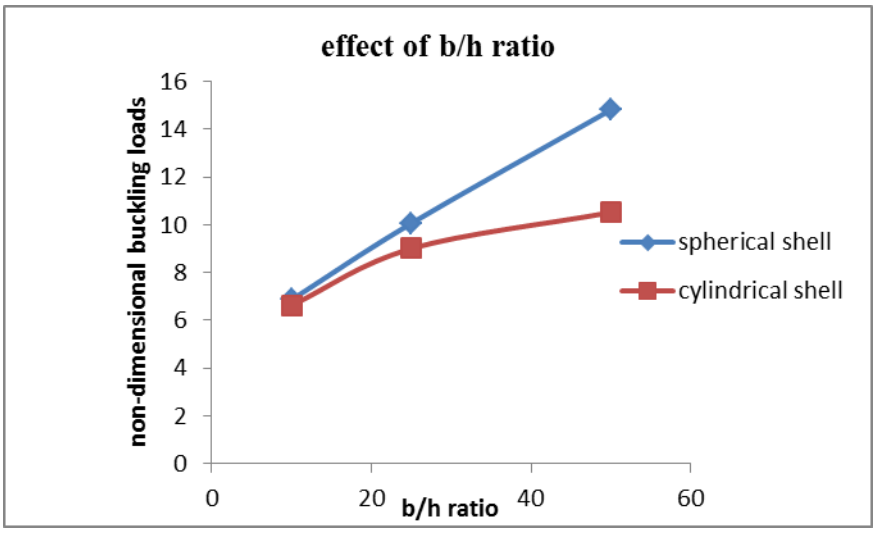


**Figure 11:** Variation of non-dimensional buckling load vs. b/h ratio for simply supported composite shell. $R_x/a=5$, $R_y/a=5$, cross-ply-$(0/90)_n$ .

**Table 4.5:** Variation of non-dimensional buckling load with different b/h ratio for 0% delaminated composite shell. $R_x/a=10$, $R_y/a=10$, $E_1=10E_2$, cross-ply-(0/90/0/90/0)

| b/h | Spherical shell | Cylindrical shell |
|---|---|---|
| 10 | 6.6183 | 6.6249 |
| 25 | 9.0448 | 8.7832 |
| 50 | 10.5710 | 9.5276 |

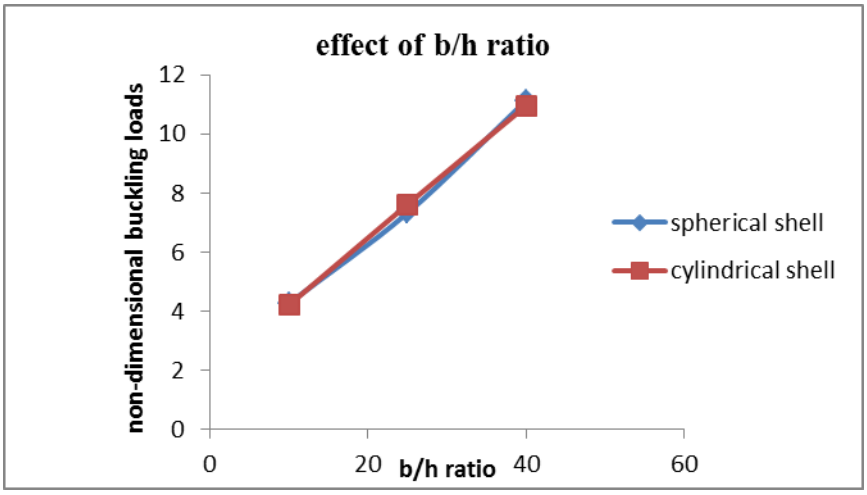


**Figure 12:** Variation of non-dimensional buckling load vs. b/h ratio for simply supported composite shell. $R_x/a=5$, $R_y/a=5$, cross-ply-$(0/90)_n$ .

Numerical result of non-dimensional buckling load with different degree of orthotropic for 0% delamination composite shell is presented in table 4.6 and table 4.7. Variations of non-dimensional buckling load with different degree of orthotropy shown in fig13 and fig14. It observed that as degree of orthotropic increases the non-dimensional buckling load increases.

**Table 4.6:** Variation of non-dimensional buckling load with different degree of orthotropic for 0% delaminated composite shell. $R_x/a=5$, $R_y/a=5$, $a/h=10$, cross-ply-(0/90/0/90/0)

| $E_1/E_2$ | Spherical shell | Cylindrical shell |
|---|---|---|
| 10 | 4.5802 | 4.2659 |
| 25 | 8.2576 | 7.7389 |
| 40 | 11.9450 | 11.1458 |

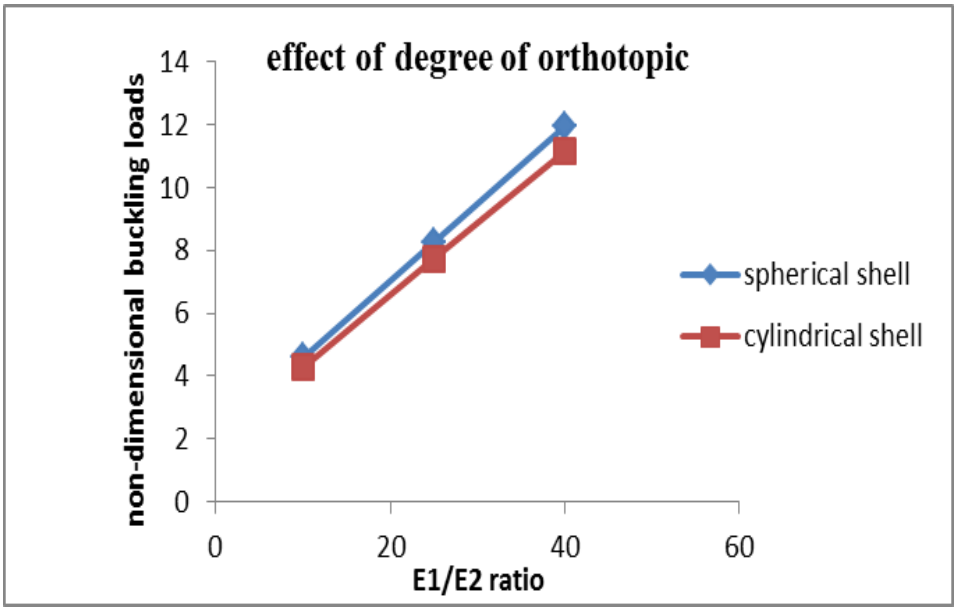


**Figure 13:** Variation of non-dimensional buckling load vs. $E_1/E_2$ ratio for simply supported composite shell. $R_x/a=5$, $R_y/a=5$,

**Table 4.7:** Variation of non-dimensional buckling load with different $E_1/E_2$ ratio for 0% delaminated composite shell. $R_x/a=10$, $R_y/a=10$, a/h=10, cross-ply-(0/90/0/90/0).

| $E_1/E_2$ | Spherical shell | Cylindrical shell |
|---|---|---|
| 10 | 4.2730 | 4.2149 |
| 25 | 7.3335 | 7.6197 |
| 40 | 11.1338 | 10.9569 |

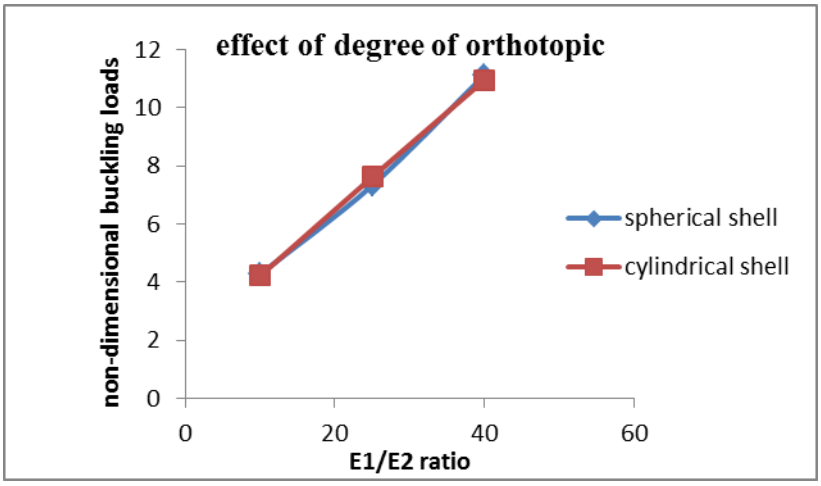


**Figure 14:** Variation of non-dimensional buckling load vs. $E_1/E_2$ ratio for simply supported composite shell. $R_x/a=5$, $R_y/a=5$,

Numerical results of non-dimensional buckling load with different no of layers for 6.25%, 25% and 56.25% delaminated composite plate and shell with different curvature are presented in Table 4.8, Table 4.9, and Table 5.1. The variation of non-dimensional buckling load with different no of layers with different % of delamination is presented in fig 15, fig 16, and fig 17. It observed that as no of layers increases the non-dimensional buckling load increases for each delamination case and it also investigated that as % of delamination increases the non-dimensional buckling load decreases.

**Table4.8:** Variation of non-dimensional critical buckling load with different no. of layers for different percentage of delaminated composite shell. $R_y/a=10$. Cross-ply-$(0/90)_n$

| No of layers | Delamination % | | |
|---|---|---|---|
| | 6.25% | 25% | 56.25% |
| 2 | 11.0223 | 10.1426 | 9.3741 |
| 4 | 14.7349 | 7.8369 | 4.7022 |
| 8 | 18.5797 | 11.7883 | 8.5228 |

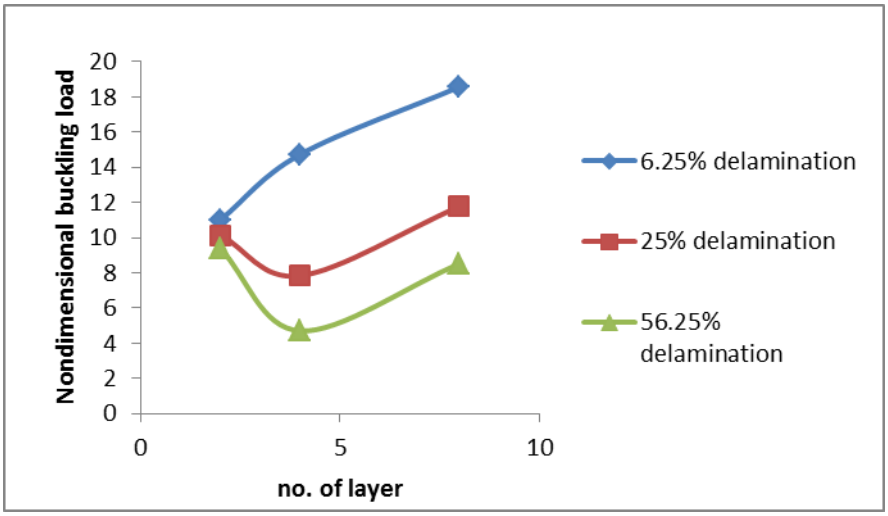


**Figure 15:** Variation of non-dimensional buckling load vs. no. of layers for simply supported composite shell with different % of delamination. $R_y$ =2, cross-ply-$(0/90)_n$

**Table4.9:** Variation of non-dimensional critical buckling load with different no. of layers for different percentage of delaminated composite shell. $R_x/a=5$, $R_y/a=5$ cross-ply-$(0/90)_n$

| No of layers | Delamination % | | |
|---|---|---|---|
| | 6.25% | 25% | 56.25% |
| 2 | 11.5480 | 10.6895 | 9.3741 |
| 4 | 15.2722 | 8.3798 | 4.7022 |
| 8 | 9.9338 | 5.2532 | 9.0993 |

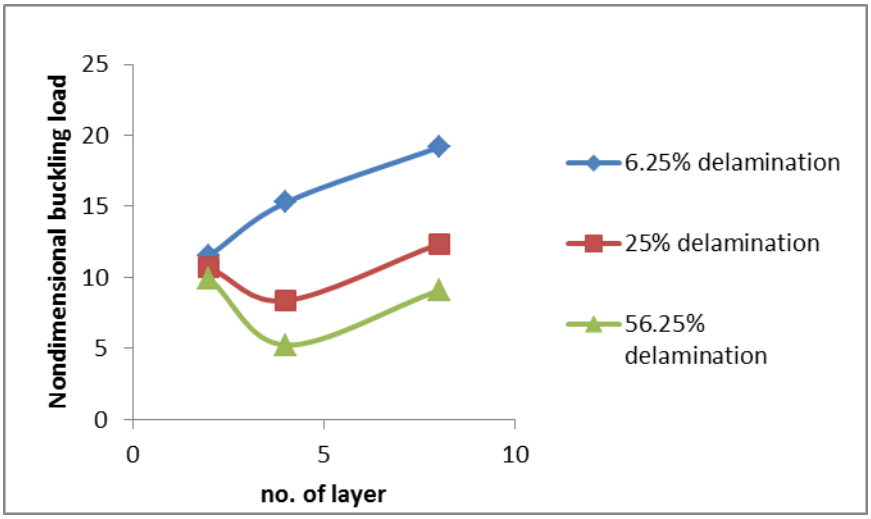


**Figure 16:** Variation of non-dimensional buckling load vs. no. of layers for simply supported composite shell with different % of delamination. $R_x/a=5$, $R_y/a=5$, cross-ply-$(0/90)_n$

**Table5.1:** Variation of non-dimensional critical buckling load with different no. of layers for different percentage of delaminated composite plate. Cross-ply $(0/90)_n$

| No of layers | Delamination % | | |
|---|---|---|---|
| | 6.25% | 25% | 56.25% |
| 2 | 12.6494 | 9.8011 | 9.0518 |
| 4 | 14.9647 | 7.5238 | 8.6562 |
| 8 | 18.3863 | 11.5318 | 8.2304 |

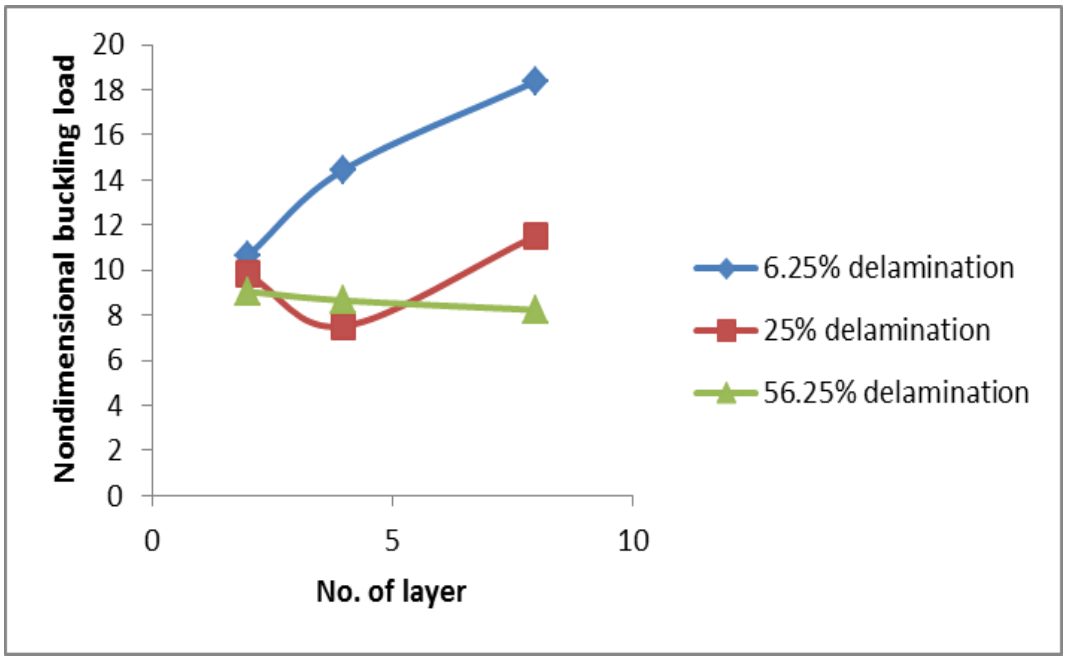


**Figure17:** Variation of non-dimensional buckling load vs. no. of layers for simply supported composite plate with different % of delamination. Cross-ply-$(0/90)_n$

Numerical results of non-dimensional buckling load with different side to thickness ratio for 6.25%, 25% and 56.25% delaminated composite plate and shell with different curvature are presented in Table5.2. The variation of non-dimensional buckling load with different b/h ratios with different % of delamination is presented in fig 18. It observed that as b/h ratio increases the non-dimensional buckling load increases for each delamination case and it also investigated that as % of delamination increases the non-dimensional buckling load decreases.

**Table5.2:** Variation of non-dimensional critical buckling load with different b/h ratio for different percentage of simply supported delaminated composite plate. Cross-ply-(0/90)

| b/h | Delamination % | | |
|---|---|---|---|
| | 6.25% | 25% | 56.25% |
| 10 | 10.6494 | 9.8011 | 9.0518 |
| 20 | 11.8513 | 10.7830 | 9.8596 |
| 50 | 12.3561 | 11.1885 | 10.2022 |

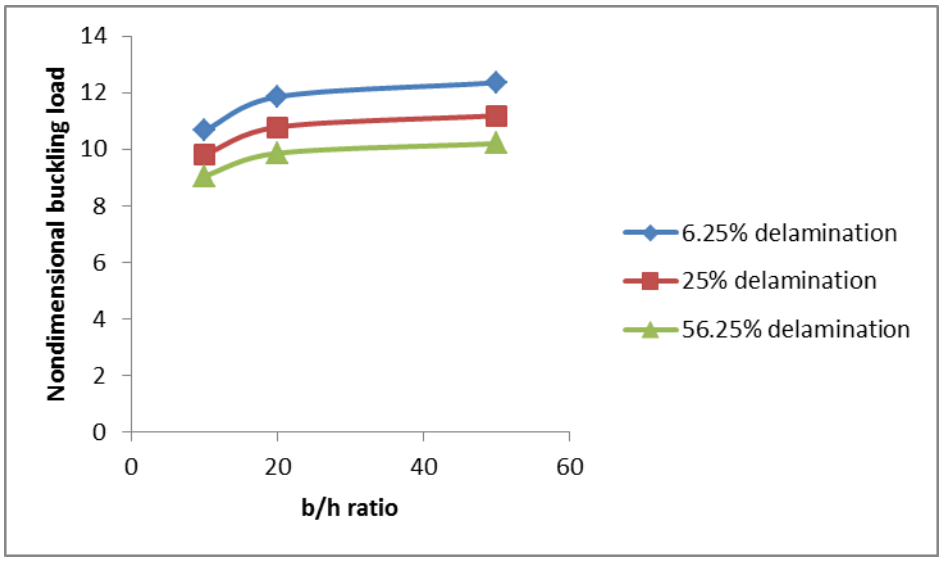


**Figure 18** Effect of % of delamination on non-dimensional critical buckling with varying b/h ratio.

## Numerical result for dynamic stability

Dynamic instability region are plotted for rectangular plates of stacking sequence $[(0/90)_2]_s$ for different delamination length. The laminates are made out of eight identical plied with material properties:

$\rho = 1600kg/m^3$,
$E_{11} = 134.4GPa.\ E_{22} = 10.34GPa,\ G_{12} = G_{13} = 4.999GPa,\ G_{23} = 1.999GPa$ .

a= 127mm, b=12.7mm, t=1.016mm, stacking sequence= (0/90/0/90/90/0/90/0).

In this study the boundary conditions is one of the short edges fixed and opposite edge loaded with dynamic buckling force. The non-dimensional excitation frequency $\Omega = \bar{\Omega}a^2\sqrt{\rho/h^2}\,E_2$ used throughout the dynamic instability studies. Where $\bar{\Omega}$ is the excitation frequency in radian /second.

The effect of delamination on instability regions for length to thickness ratio (L/t =125 and 25) is shown in fig19 and fig 20. The onset of dynamic instability regions occurs later for 0% delamination.

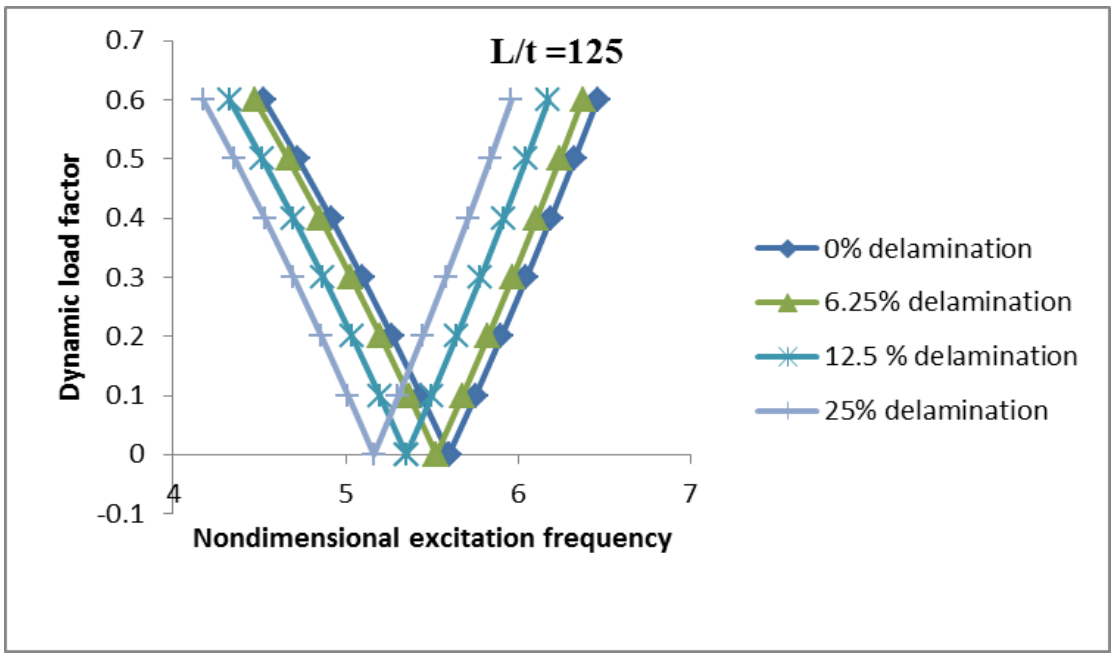


**Fig19.** Effect of delamination on instability region of $[(0/90)_2]_s$ cross- ply plate for L/t =125

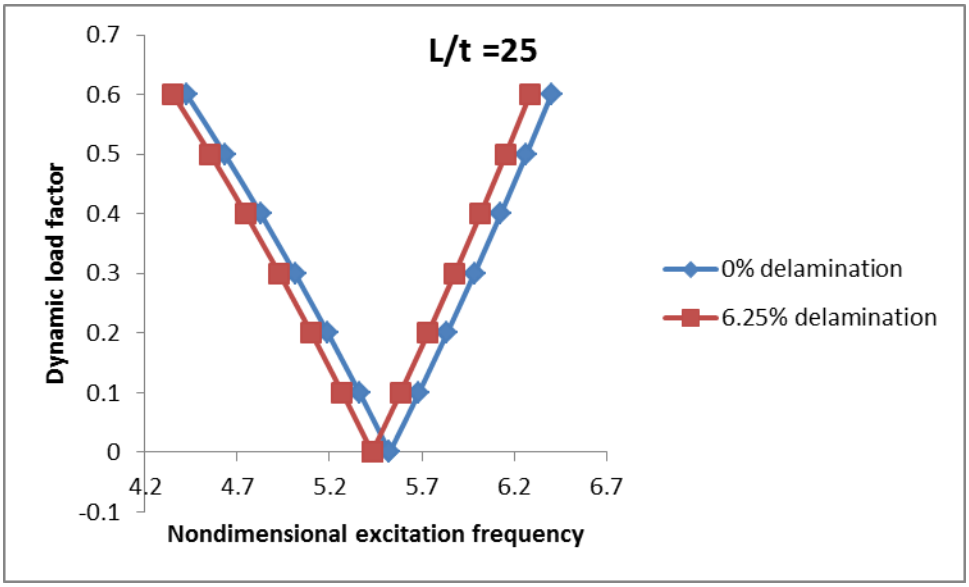


**Fig20**. Effect of delamination on instability region of $[(0/90)_2]_s$ cross- ply plate for L/t =25

The effect of delamination for different no of layers is shown in fig 21 and fig 22. Dynamic instability regions are plotted for 2 and 4 layer cross-ply rectangular plate. For both the cases instability regions occurs later for 0% delamination.

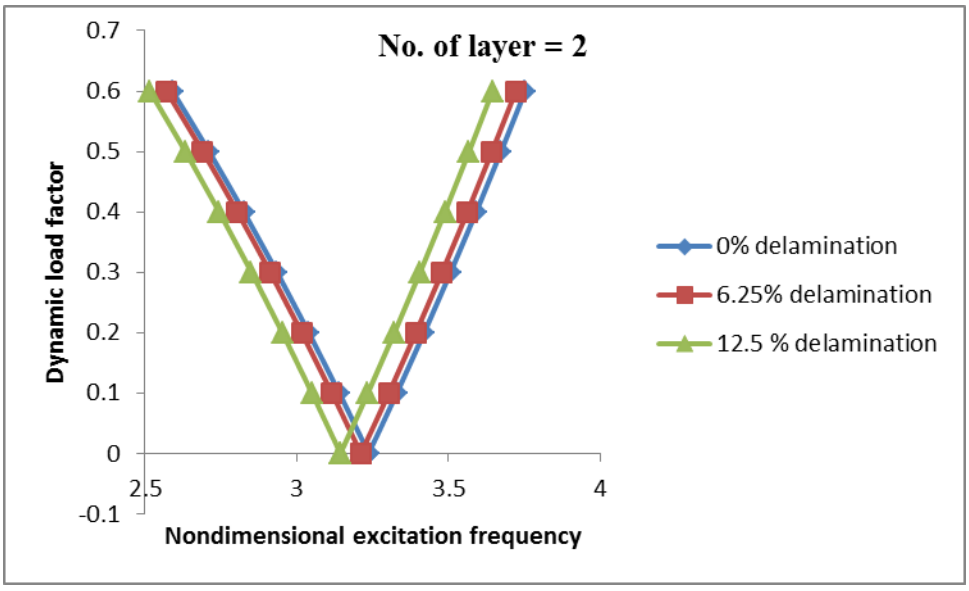


**Fig21**. Effects of % of delamination on instability region of 2-layer cross-ply delaminated plates.

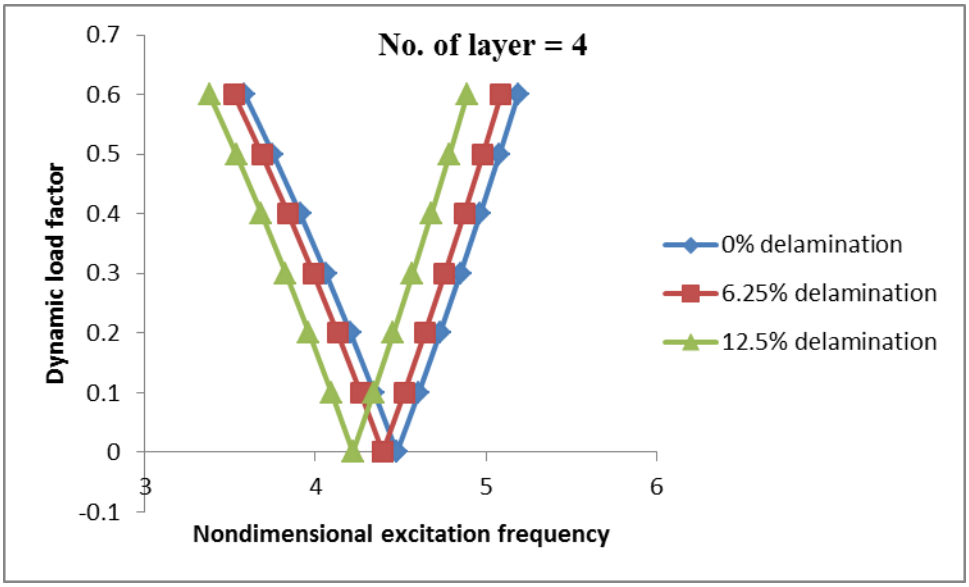


**Fig22.** Effect of % of delamination on instability region for 4-layer cross-ply delaminated plate.

The effect of delamination is studied for degree the orthotropic $E_{11}/E_{22}$ =40 and 20, and keep the other material parameters constants is shown in fig 23 and fig 24. Both the cases instability regions occur later at 0% delamination.

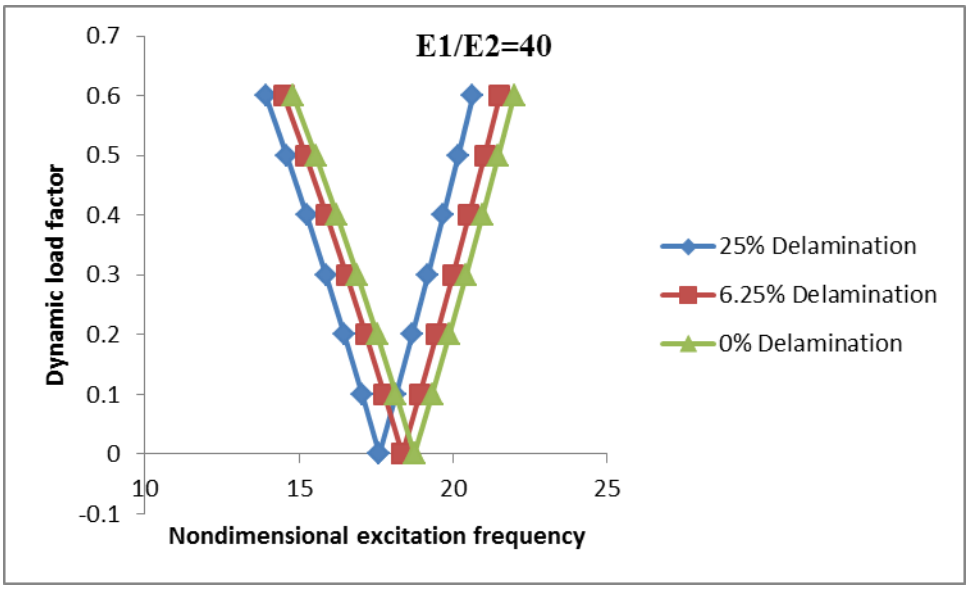


**Fig23**. Effect of % of delamination on instability region for cross ply delaminated plate for degree of orthotropy, $E_{11}/E_{22}$ =40.

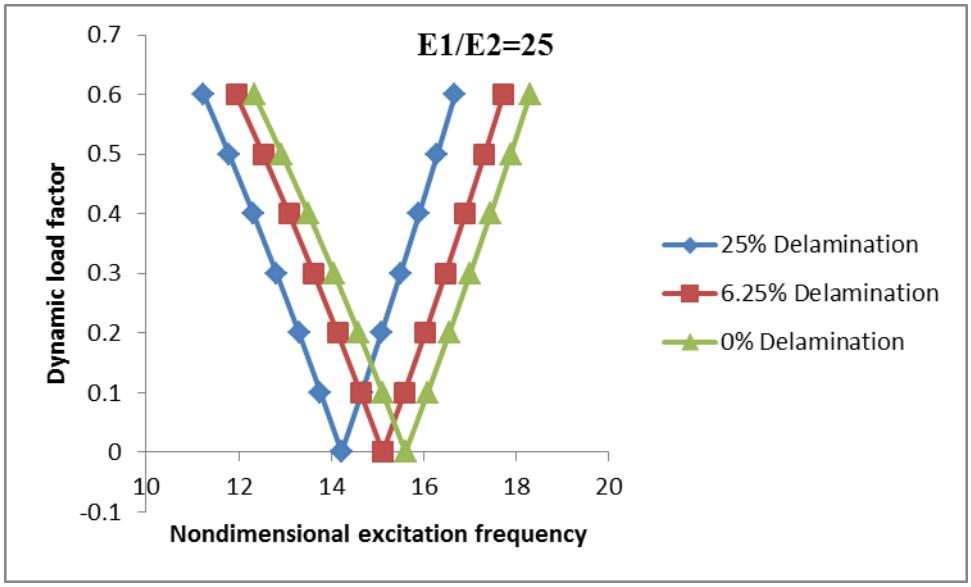


**Fig 24:** Effect of % of delamination on instability region for cross ply delaminated plate for degree of orthotropy, $E_{11}/E_{22}$ =20.

Fig 25 and fig 26 Shows the effect of aspect ratio on instability region at 0% and 25% delamination. It is observed that the onset of dynamic instability occurs much later with increase of the aspect ratio and increasing width of instability regions.

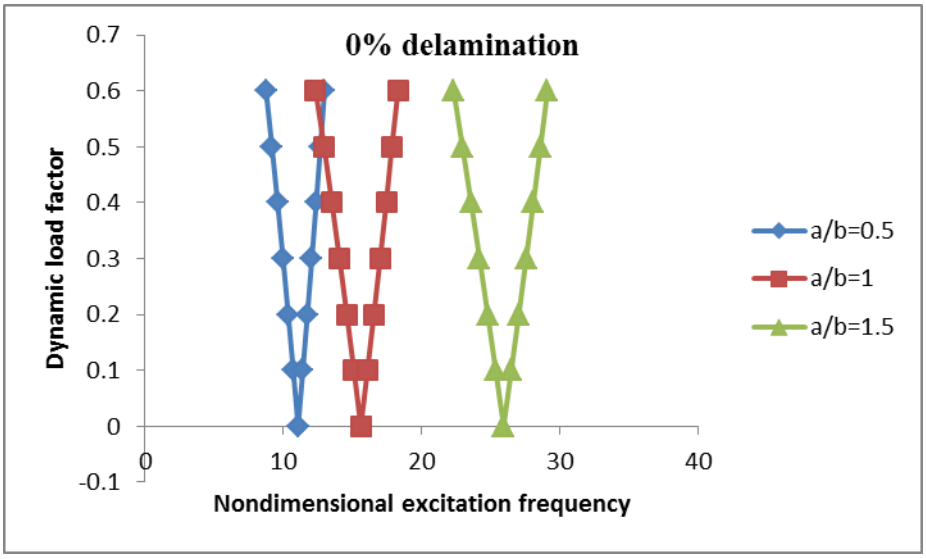


**Fig 25:** Effect of aspect ratio on instability region for simply supported cross ply delaminated plate. L/t=10**,** $E_1/E_2 = 25$, $\boldsymbol{\alpha}$=0.2.

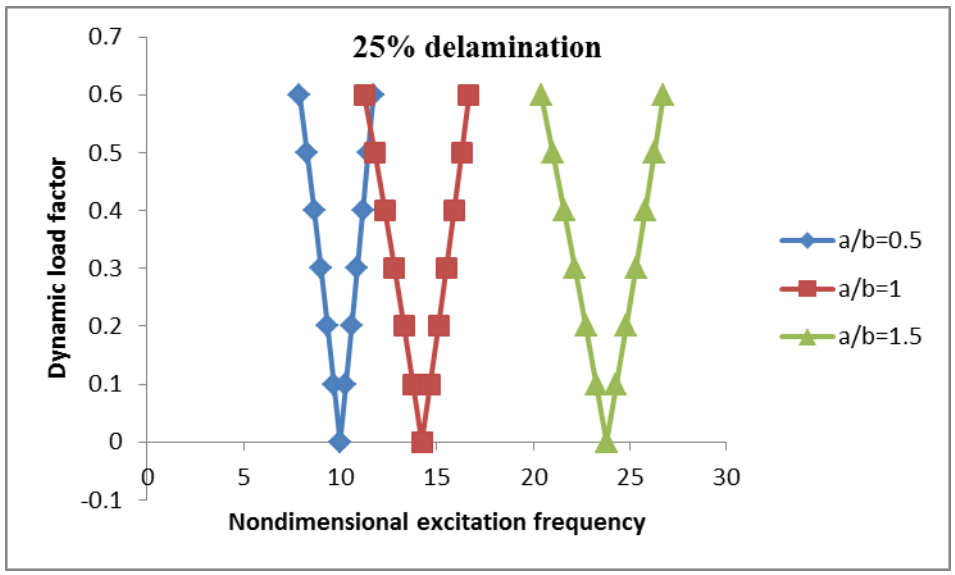


**Fig 26:** Effect of aspect ratio on instability region for simply supported cross ply delaminated plate. L/t=10**,** $E_1/E_2 = 25$, $\boldsymbol{\alpha}$=0.2.

The effect of static component of load for α = 0.0, 0.2 and 0.4 on instability region is shown in fig 27. A clamped-free-clamped-free boundary condition has taken into account in this study with 6.25% delamination. Due to increase of static component the instability regions tends to shift to lower frequencies and become wider.

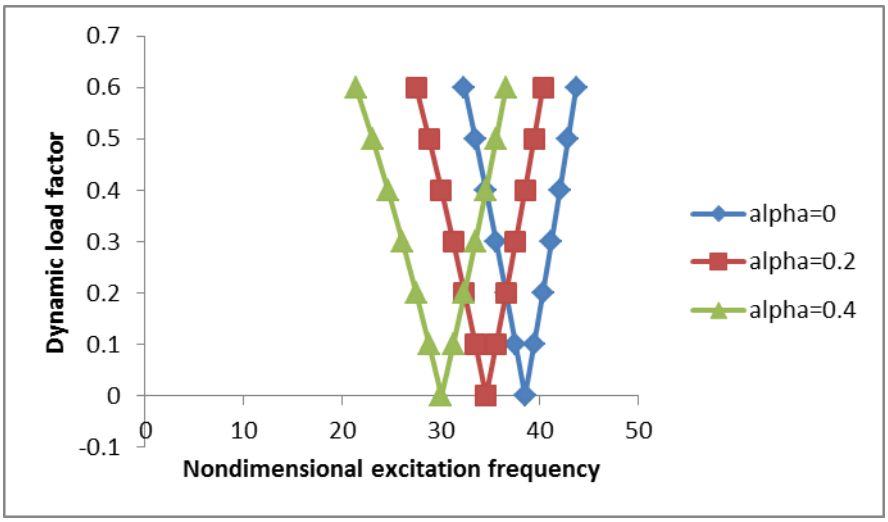


**Fig27**. Effect of static load factor on instability region of rectangular plate (127*12.7*1.016)mm. $\rho = 1600kg/m^3$,

$E_{11} = 134.4GPa.\ E_{22} = 10.34GPa,\ G_{12} = G_{13} = 4.999GPa,\ G_{23} = 1.999GPa$ .

a= 127mm, b=12.7mm, t=1.016mm, stacking sequence= (0/90/0/90/90/0/90/0).

Fig 28 and fig 29 shows the dynamic instability regions for delaminated spherical shell at different % of delamination. It is observed that the onset of dynamic instability occurs later with decrease of delamination.

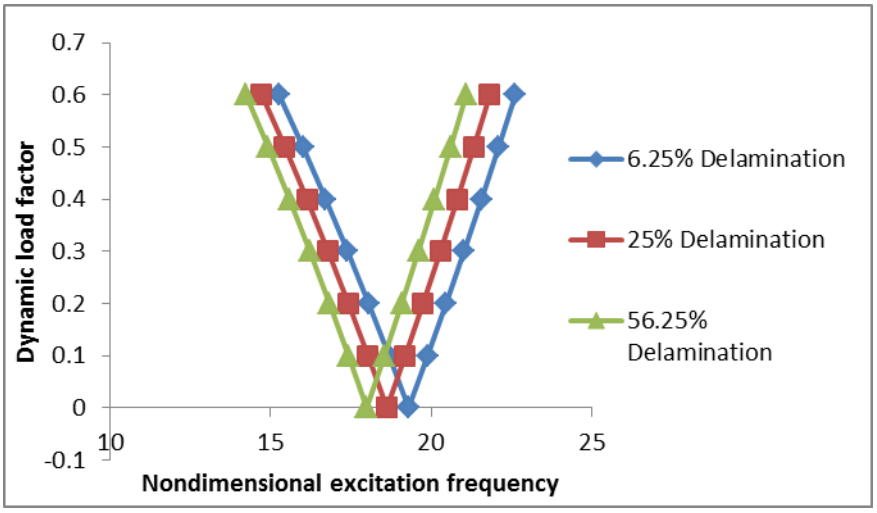


**Fig28.** Effect of % of delamination on the instability region of simply supported cross ply (0/90) spherical shell: $a/R_x = b/R_y = 0.25$, $\alpha = 0.2$, $a/b = 1$, $a/h = 10$, $E_{11} = 40E_{22}$, $G_{12} = G_{13} = 0.6E_{22}$, $G_{23} = 0.5E_{22}$, $\vartheta_{12} = \vartheta_{23} = 0.25$.

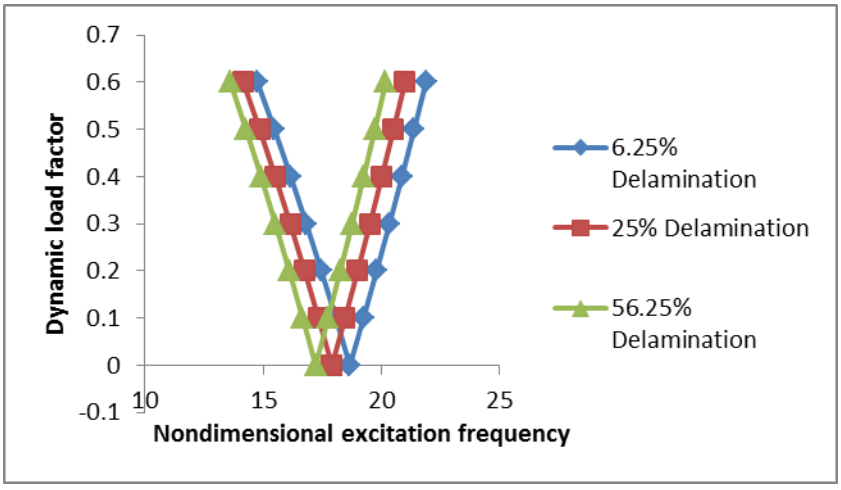


**Fig29**. Effect of % of delamination on the instability region of simply supported cross ply (0/90) cylindrical shell: $b/R_y = 0.25$, $\alpha = 0.2$, $a/b = 1$, $a/h = 10$, $E_{11} = 40E_{22}$, $G_{12} = G_{13} = 0.6E_{22}$, $G_{23} = 0.5E_{22}$, $\vartheta_{12} = \vartheta_{23} = 0.25$.

The effect of curvature on instability region with 6.25% and 25% of delamination of simply supported cross ply shown in fig 30 and fig 31. It shows in fig that the dynamic instability occurs earlier in case of plate with increase of delamination.

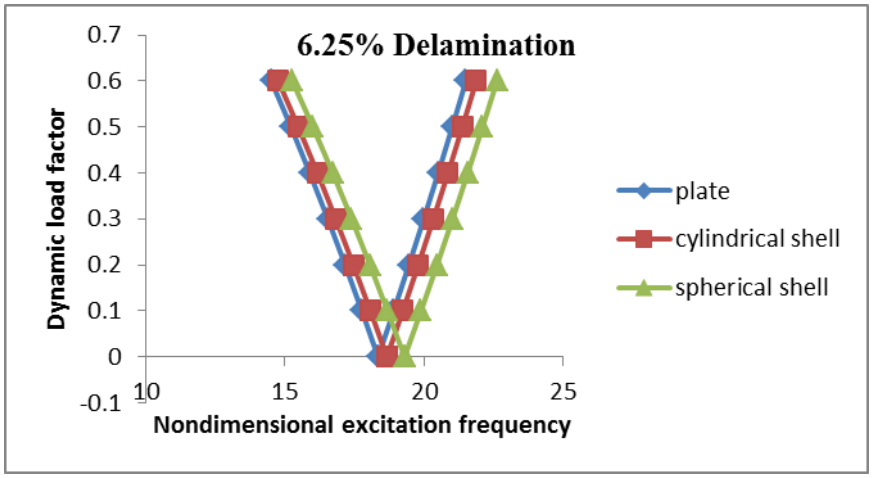


**Fig30** Effect of curvature on instability region with 6.25% of delamination of simply supported cross ply (0/90): $a/R_x=b/R_y=0.25$, $\alpha=0.2$, $a/b=1$, $a/h=10$, $E_{11}=40E_{22}$, $G_{12}=G_{13}=0.6E_{22}$, $G_{23}=0.5E_{22}$, $\vartheta_{12}=\vartheta_{23}=0.25$.

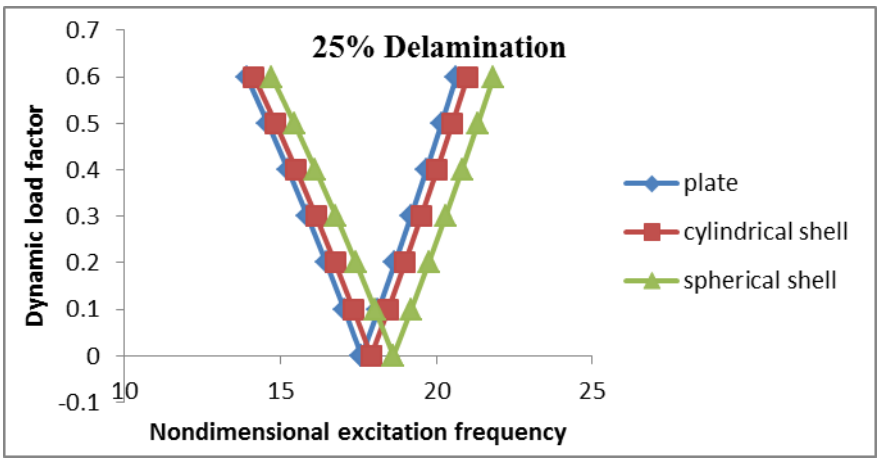


**Fig31** Effect of curvature on instability region with 25% of delamination of simply supported cross ply (0/90): $a/R_x = b/R_y = 0.25$, $\alpha=0.2$, $a/b=1$, $a/h=10$, $E_{11}=40E_{22}$, $G_{12}=G_{13}=0.6E_{22}$, $G_{23}=0.5E_{22}$, $\vartheta_{12}=\vartheta_{23}=0.25$

# CHAPTER 5

## CONCLUSION

A first order shear deformation theory based on finite element model has been developed for studying the instability region of mid plane delaminated composite plate and shell.

The following observations are made from this study:-

**Vibration study**

- The effects of dynamic behaviour on delaminated composite plates and shells under free vibration conclude that for particular % of delamination, the natural frequencies increase with increase of number of layers due to effect of bending-stretching coupling.
- With increase of aspect ratio, the natural frequency decreases.
- With increase of % delamination, the natural frequency decreases and it also observed the frequency of vibration increase with decrease of b/h ratio of cross ply panels with delamination. This is due to reduction in stiffness caused by delamination.
- With increase of % delamination the natural frequency decreases with different degrees of orthotropic.
- The frequency of vibration increases with increase of degree of orthotropy due to increase of stiffness.

**Buckling study**

- If no. of layers increases the non-dimensional buckling load increases and it also investigated that as % of delamination increases the non-dimensional buckling load decreases.

- If b/h ratio increases the non-dimensional buckling load increases for each delamination case and it also investigated that as % of delamination increases the non-dimensional buckling load decreases.
- The natural frequencies and the non-dimensional buckling load decrease with increase in delamination length. This is due to the reduction in stiffness caused by delamination.
- With increase of degree of orthotropic the buckling load increases and it also observed that buckling load increase with decrease of delamination.

**Dynamic stability study**

- The onset of instability occurs earlier with increase in percentage of delamination.
- It also observed that with increases of number of layers the excitation frequency increases. This is due to increase of stiffness caused by bending-stretching coupling with increase of layers.
- The dynamic instability region occurs earlier with decrease of degree of orthotropy and due to decrease of delamination the onset instability region shifted to lower frequency to higher frequency and also the width of instability regions increased with decrease of delamination.
- The dynamic instability occurs much later with increase of aspect ratio and width of instability region increase with increase of aspect ratio for delaminated cross ply panel.
- With increase of static load factor the instability region tends to shift to lower frequencies and become wider showing destabilizing effect on the dynamic stability behaviour of delaminated composite plate.

- It observed that the onset of instability occurs at higher load frequencies with the introduction of curvatures when compared with the flat member. This is probably due to the influence of increased stiffness of shells. The onset of load frequency is heavily dependent on the radius to length ratio.

**Further scope of study:**

In the Present study, natural frequency, buckling load and dynamic stability of delaminated cross-ply composite plate and shell was determined numerically. The effect of various parameters like percentage of delamination area, number of layers, aspect ratio, degree of orthotropy and different side to thickness ratio was studied. The future scope of the present study can be extending as follows:

- Dynamic stability of multiple delaminated plate and shell can be studied.
- The present study is based on linear range of analysis. It can also extend for nonlinear analysis.
- Dynamic stability of composite plates with circular, elliptical, triangular shaped delamination can be studied.
- The effect of damping on instability regions of delaminated composite plates and shells can be studied.

# CHAPTER 6

## REFERENCES


**Abdullah[a,]*,Ferrero[b],Barrau[b],and Mouillet[c]**,(2007),"Development of a new finite element for composite delamination analysis" *Composites Science and Technology* 67, 2208–221.

**Alnefaie,** (2009), "Finite element modeling of composite plates with internal delamination" *Composite Structures* 90, 21–27.

**Bert, C.W. and Birman, V.** (1988) "Parametric instability of thick orthotropic circular cylindrical shells". *Acta Mechanica*, 71,61-76,.

**Bolotin VV** (1964), *The Dynamic stability of elastic systems*, Holden-Day, San Francisco.

**Chang, Hu, and Jane**, (1998), The vibration analysis of a delaminated composite plate under axial load**,** *Mech. Struct. & Mach*, 26(2), 195-218.

**Chen *, Hong, and Liu**, (2004), the dynamic behavior of delaminated plates considering progressive failure process. *Composite Structures* 66, 459–466

**Chirica, Elena-Felicia and Beznea**, (2010), "Buckling analysis of the composite plates with delaminations" *Computational Materials Science* 50,1587–1591.

**Geubelle* and Baylor**, (1998), "Impact-induced delamination of composites using a 2D simulation" *Composites Part B* 29B, 589–602.

**Houa,*,and Jeronimidisb** , (1999), "Vibration of delaminated thin composite plates" *Composites: Part A* 30 ,989–995.

**Hu, Fukunaga, Kameyama, Aramaki, and Chang,** (2002), Vibration analysis of delaminated composite beams and plates using a higher-order finite element, *International Journal of Mechanical Sciences* 44 1479–1503

**Hwang* and Mao,(**2001) "Failure of Delaminated Carbon/Epoxy Composite Plates under Compression" *Journal of Composite Materials* 35; 1634.

**Ju-fen, Gang, Howson and Williams**, (2003), "Reference surface element modelling of composite plate/shell delamination buckling and postbuckling" *Composite Structures 61* 255–264

**Ju, Lee and Lee,** (1995), "Finite element analysis of free vibration of delaminated composite plates" *Composites Engineering*, Vol. 5, No. 2, pp. 195-209

**Ju, .Lee and .Lee** (1995) "Free vibration of composite plates with delamination around cut-outs" *Composite Structure*, 31,177-183

**KüÇük,** (2004), an investigation on buckling behaviour of simply supported woven steel, Reinforced thermoplastic laminated plates with lateral strip delamination. *Journal of Reinforced Plastics and Composites* 23; 209

**Lee and Chung**,(2010), " Finite element delamination model for vibrating composite spherical shell panels with central cut-outs" *Finite Elements in Analysis and Design* 46 247–256.

**Librescu, Khdeir and Frederick.** ,(1989). Shear deformation theory of laminated composite of shallow shell type panels and their response analysis. I: Free vibration and buckling. *Acta Mechnica*, 76, 1-33

**Oh, Cho *and* Kim,** (2008)," Buckling analysis of a composite shell with multiple delaminations based on a higher order zig-zag theory" *Finite Elements in Analysis and Design* 44 ,675 – 685.

**Ovesy and Kharazi,** (2011), "Stability analysis of composite plates with through-the-width delamination". *Journal Of Engineering Mechanics © ASCE*. 87-100.

**Ostachowicz and Kaczmarezyk**, (2001), "vibration of composite plates with SMA fibres in a gas stream with defects of the type of delamination*". Composite structure 54*,305-311.

**Park and Lee,** (2009),"Parametric instability of delaminated composite spherical shells subjected to in-plane pulsating forces" *Composite Structures* 91,196–204.

**Parhi, Bhattacharyya and Sinha**, (2001), "Hygrothermal effects on the dynamic behavior of multiple delaminated composite plates and shells" *Journal of Sound and vibration* 248(2), 195-214.

**Radu and Chattopadhyay**, (2002), "Dynamic stability analysis of composite plates including delaminations using a higher order theory and transformation matrix approach" *International journals of solids and structures*, volume 39, issue 7,April 2002,Pages 1949-1965.

**Sahu and Dutta,** (2001),"Parametric Resonance Characteristics of Laminated Composite Doubly Curved Shells Subjected to Non-Uniform Loading". *Journal Of Reinforced Plastics And Composites*. Vol 20, Iss 18.

**Sciuva, M.D and Carrere E.** (1990), Static buckling of moderately thick anisotropic, laminated and sandwich, cylindrical shell. *AIAA Journal*,28,1782-1793.

**Shan and Pelegri**,(2003),"Approximate Analysis of the Buckling behaviour of Composites with Delamination" *Journal of Composite Material*, 37, 673

**Tafreshi,**(2006),"Delamination buckling and postbuckling in composite cylindrical shells under combined axial compression and external pressure" *Composite Structures* 72,401–418.

**Tenek,"* ,Henneke II ° & Gunzburger b**. (1993), "vibration of delaminated composite plates and some applications to non-destructive testing" *Composite Structures* 23, 253-262.

**Williams and Addessio,** (1998), A dynamic model for laminated plates with delaminations, *Int. J. Solids Structures VoL* 35, Nos. 1-2, pp. 83-106,

.**Wang, Su, Lu and Wang**, (2003), "Non-Linear Thermal Buckling for Local Delamination near the Surface of Laminated Plates" *Journal of Reinforced Plastics and Composites* ; 22; 419.

**Yang and Fu,** (2006) "Delamination growth of laminated composite cylindrical shells" Theoretical and Applied Fracture Mechanics 45, 192–203. *Composite Structures* 78,309–315.

**Yang and Fu**[a], (2007), "Analysis of dynamic stability for composite laminated cylindrical shells with delaminations" *Composite structures*, volume 78 , issue 3 , pages 309-315.

# APPENDIX

**Delamination Modelling:**

For Single mid-plane delamination with different sizes like 0, 6.25%, 25%, 56.25% of the total plate area is considered. The delamination sizes are assumed to increase from the centre of the laminate and can be located anywhere along the thickness of the laminate. The composite plates with different percentage of delamination are shown in figure 8.1 to 8.4.

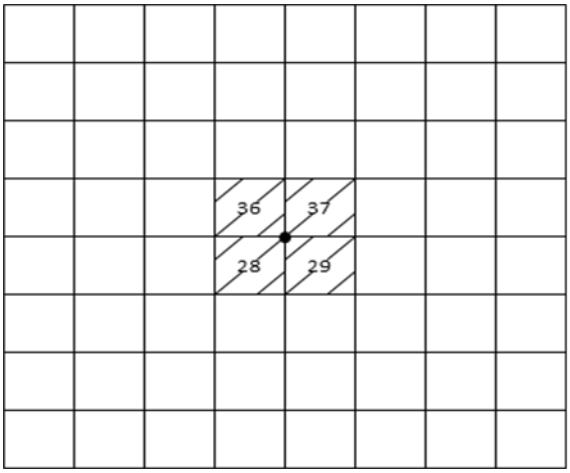


**Figure 32:** 6.25% central delamination

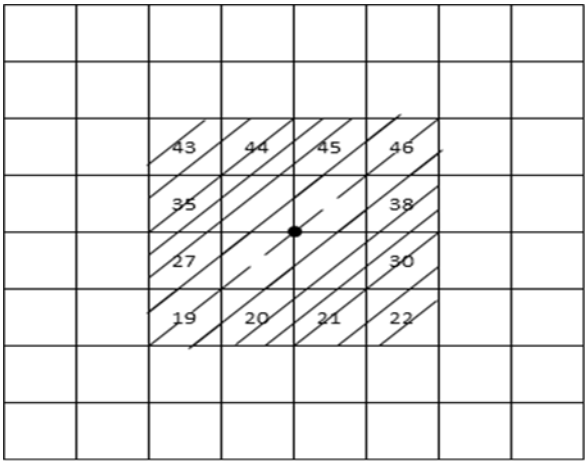


**Figure 33:** 25% central delamination

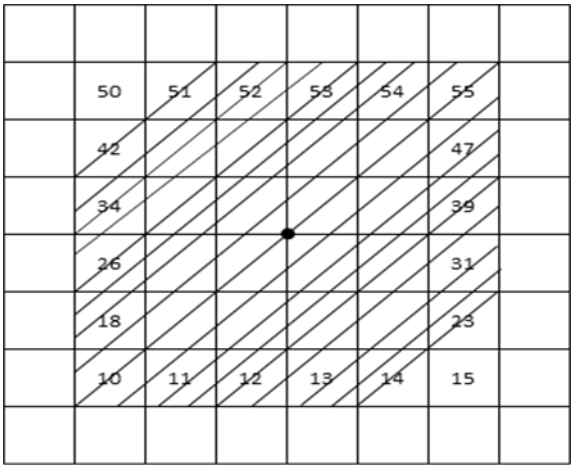


**Figure 34:** 56.25% central delamination

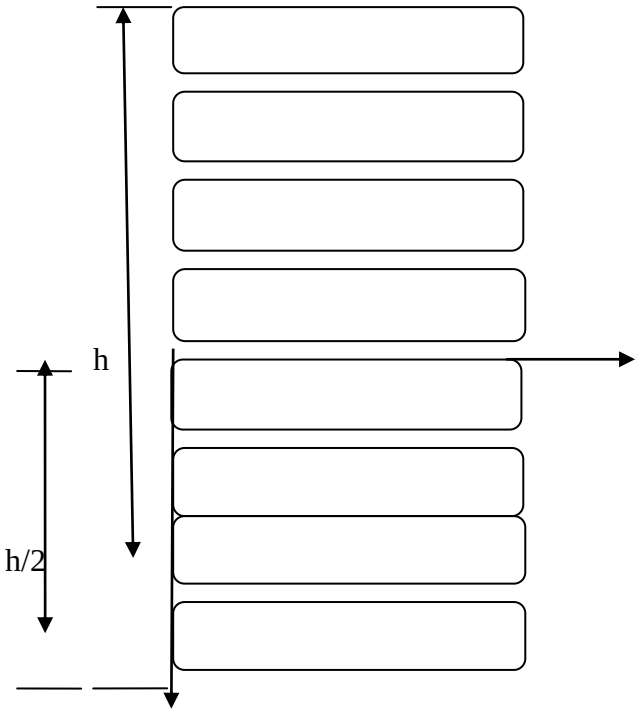


**Figure 35:** Eight layered laminate without delamination

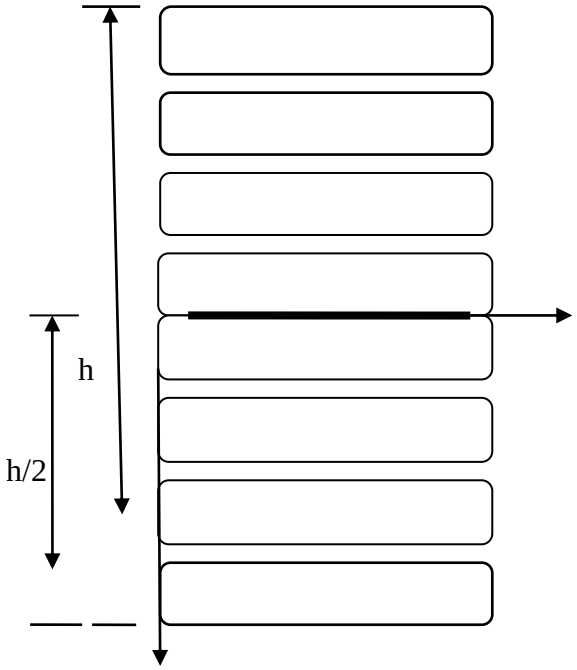


**Figure 36:** Eight layered laminate with mid-plane delamination

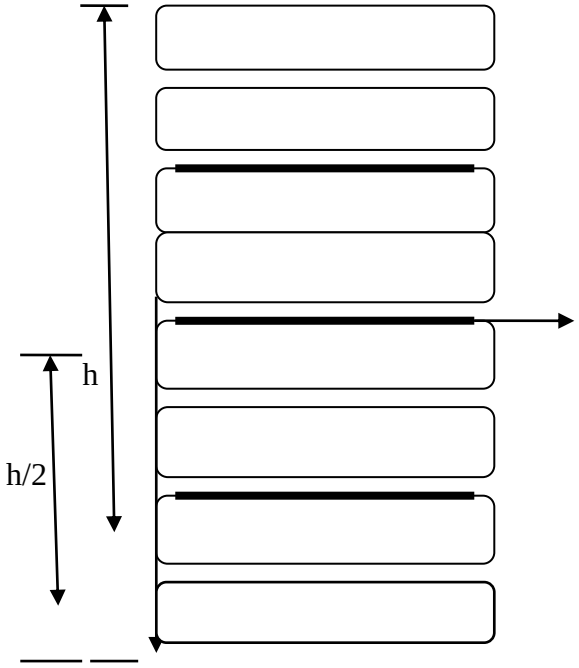


**Figure 37:** Eight layered laminate with three delaminations